Hindawi Publishing Corporation
Mathematical Problems in Engineering
Volume 2016, Article ID 3196958, 24 pages
http://dx.doi.org/10.1155/2016/3196958

Research Article

Improved Glowworm Swarm Optimization Algorithm for Multilevel Color Image Thresholding Problem

Lifang He[1] and Songwei Huang[2]

[1]*Department of Electronics and Communication Engineering, Kunming University of Science and Technology, Kunming 650093, China*
[2]*Department of Mineral Processing, Kunming University of Science and Technology, Kunming 650093, China*

Correspondence should be addressed to Lifang He; 843168660@qq.com

Received 12 May 2016; Revised 22 July 2016; Accepted 27 July 2016

Academic Editor: Masoud Hajarian

The thresholding process finds the proper threshold values by optimizing a criterion, which can be considered as a constrained optimization problem. The computation time of traditional thresholding techniques will increase dramatically for multilevel thresholding. To greatly overcome this problem, swarm intelligence algorithm is widely used to search optimal thresholds. In this paper, an improved glowworm swarm optimization (IGSO) algorithm has been presented to find the optimal multilevel thresholds of color image based on the between-class variance and minimum cross entropy (MCE). The proposed methods are examined on standard set of color test images by using various numbers of threshold values. The results are then compared with those of basic glowworm swarm optimization, adaptive particle swarm optimization (APSO), and self-adaptive differential evolution (SaDE). The simulation results show that the proposed method can find the optimal thresholds accurately and efficiently and is an effective multilevel thresholding method for color image segmentation.

1. Introduction

Image segmentation is to partition an image into multiple segments or regions and extract the meaningful and interested objects, which is the critical step in image processing and image analysis. The goal of image segmentation is to make an image more meaningful and easier to understand and analyze [1, 2]. Nowadays image segmentation has been widely used in many practical applications such as medical imaging [3], object detection [4], optical character recognition (OCR) [5], and remote sensing [6].

By now, several algorithms and techniques have been proposed for image segmentation in the literature and thresholding is one of the simplest but most effective methods in all the image segmentation algorithms. The fundamental principle of thresholding technique is to divide the whole pixel points of an image into several classes by setting different threshold values, so the key to this method is to find the proper threshold values. According to the number of threshold values, thresholding techniques can be separated into two groups: bilevel and multilevel thresholding. Bilevel thresholding is to divide an image into two parts by using one threshold value. If the threshold value is more than one, it will be extended into multilevel thresholding, which can accurately divide an image into several significant parts. Therefore, multilevel thresholding is an effective and famous technique, and it is extensively applied in many fields.

For years, a great number of thresholding techniques have been described in the literature. In 1979, Otsu's method was presented by Otsu [7], which is one of the best ways of thresholding. However, the computation time is much longer in multilevel threshold problem because it exhaustively searches optimal threshold values by maximizing the between-class variance. In 1985, Tsai [8] proposed a new method to find optimal thresholding values of an input gray-level image by moment-preserving principle, which is called Tsallis entropy method. In 1986, Kittler and Illingworth [9] assumed that the pixel level values of each object in an image are normally distributed. Li and Lee [10] proposed minimum cross entropy thresholding method which selects the optimal thresholding values by minimizing the cross entropy between the original image and its segmented image. The Otsu, Tsallis entropy, and minimum cross entropy methods can be easily extended to multilevel thresholding. For bilevel thresholding, the traditional thresholding algorithms can find optimal threshold quickly and effectively and the image is accurately segmented into two parts. But, for multilevel thresholding, the traditional techniques become very time-consuming because a large number of iterations are needed for computing the optimal threshold values [11–13].

Swarm intelligence algorithms are very popular global optimization schemes, and the techniques imitate the collective behavior of natural or artificial systems that show some intelligence [14]. The algorithms have been widely used in complex optimization problems which show better performances. In order to solve the multilevel thresholding problem, swarm intelligence algorithms have been used to find optimal thresholds over the years, including genetic algorithm (GA) [15, 16], particle swarm optimization (PSO) [17–19], artificial bee colony (ABC) [20–22], differential evolution (DE) [23–25], firefly algorithm (FA) [26, 27], cuckoo search algorithm (CS) [28, 29], wind driven optimization (WDO) [29], and electromagnetism-like optimization (EMO) algorithm [30]. These methods use different basic swarm intelligence algorithms, different improved algorithms, and different objective functions for different types of images, such as between-class variance, Tsallis entropy, Kapur's entropy, and minimum cross entropy. GA was inspired by the process of natural selection which has been used for multilevel thresholding [31, 32]. The PSO and the improved PSO algorithms were also used to solve the multilevel thresholding problem which mimics the social behavior of bird flock or fish school. The researchers Yin [17] and Maitra and Chatterjee [18] applied PSO algorithm to multilevel thresholding. Thereafter, particle swarm optimization (PSO) and artificial bee colony (ABC) have been adopted to search the optimal multilevel thresholds by Akay using Kapur's entropy and between-class variance as objective functions [19]. Horng [20], Zhang and Wu [21], and Cuevas et al. [33] proposed a new image segmentation method using artificial bee colony algorithm for multilevel thresholding. And the algorithm is also used for segmentation of SAR image [34, 35] and satellite image [22]. In 2010, a novel multilevel thresholding segmentation method based on differential evolution (DE) algorithm is presented [23]. Firefly algorithm (FA), inspired by the social behavior of firefly swarm, is also used to find several threshold values on a given image [36]. Also, two new swarm intelligence algorithms, cuckoo search algorithm (CS) and wind driven optimization (WDO), using Kapur's entropy for multilevel thresholding are proposed, and two algorithms can efficiently and accurately search multiple threshold values [29].

Color images include more information than gray images and multilevel color image segmentation is widely used now. Swarm intelligence algorithms are also used for color image multilevel segmentation. Zingaretti et al. [37] proposed the new method which is based on genetic algorithm (GA) for color image segmentation. Raja et al. [38] presented an improved particle swarm optimization (PSO) algorithm for cancer infected breast thermal images by Otsu's method. Sarkar et al. [39] developed a novel multilevel color image thresholding method based on differential evolution (DE) algorithm and minimum cross entropy, and simulation results show that it is an effective method. Three different quantum inspired metaheuristic techniques, namely, Quantum Inspired Ant Colony Optimization, Quantum Inspired Differential Evolution, and Quantum Inspired Particle Swarm Optimization technique, for multilevel color image thresholding are presented. Simulations and results prove that the Quantum Inspired Ant Colony Optimization method outperforms the other methods [40]. Rajinikanth and Couceiro [41] used the firefly algorithm (FA) for color image segmentation. The evolutionary and swarm-based algorithms of evolution strategy (ES), genetic algorithm (GA), differential evolution (DE) algorithm, adaptive differential evolution algorithm (JADE), particle swarm optimization (PSO) algorithm, artificial bee colony (ABC) algorithm, cuckoo search (CS), and differential search (DS) algorithm are also used for multilevel color image thresholding problem [42].

The glowworm swarm optimization (GSO) is a novel swarm intelligence algorithm for optimization developed by Krishnanand and Ghose in 2005 [43] which mimics the flashing behavior of glowworms. In the algorithm, each glowworm carries a luminescence quantity called luciferin, which is decided by the function value of glowworm's current location. During the course of movement, glowworm identifies its neighbors based on local-decision domain and selects a neighbor which has a luciferin value higher than its own using a probabilistic mechanism and moves toward it [44–49]. GSO algorithm has been applied for numerous complex optimization problems. Qifang et al. [50] and Horng [51] used GSO algorithm based on Otsu's method and minimum cross entropy for multilevel threshold image segmentation and the experimental results show that the method has better performance for gray images. In order to improve the performance of the standard GSO algorithm and search the global optimal value efficiently and accurately, the improved glowworm swarm optimization (IGSO) is presented in this paper. Step size s is an important parameter in determining the convergence of GSO algorithm, so a new update method of step size is proposed. Furthermore the sensor range is extended to the whole search space and the random movement of the brightest glowworms of firefly algorithm is also introduced. Subsequently the IGSO algorithm using different objective functions is used for multilevel color image thresholding problem, such as between-class variance and minimum cross entropy (MCE). The performance of IGSO algorithm for multilevel color image thresholding is measured in terms of the optimal threshold values, objective values, the peak signal to noise ratio (PSNR), and structural similarity index (SSIM) and then compared with other swarm intelligence algorithms such as adaptive particle swarm optimization (APSO) [52] and self-adaptive differential evolution (SaDE) algorithm [53].

The remainder of the paper is organized as follows. Section 2 presents the concepts of between-class variance method and minimum cross entropy method. Section 3 gives a detailed description of GSO algorithm and the proposed IGSO algorithm. In Section 4, the numerical experimental results of IGSO, GSO, APSO, and SaDE algorithms for multilevel color image segmentation are shown and discussions are also given. Finally, the conclusion is presented in Section 5.

2. Formulation of the Problem

Swarm intelligence algorithms find the optimal thresholds by maximizing an objective function. In this paper, two commonly used thresholding methods, between-class variance method (Otsu's) and minimum cross entropy are used as objective functions to find the optimal multilevel thresholds.

2.1. Between-Class Variance Method (Otsu's Method). Thresholding based on Otsu's method is a nonparametric segmentation method that divides the whole image into classes by maximizing the between-class variance.

Assume that an image has N pixels and L gray levels, and the number of pixels at level i is represented by f_i; then $N = f_1+f_2+\cdots+f_i$. The occurrence probability of level i is defined by

$$p_i = \frac{f_i}{N}, \quad p_i \geq 0, \qquad \sum_{i=1}^{L} p_i = 1. \tag{1}$$

In bilevel thresholding, the optimum threshold t divides the image into two classes, and the cumulative probabilities of each class can be described as follows:

$$\omega_0 = \sum_{i=1}^{t} p_i, \qquad \omega_1 = \sum_{i=t+1}^{L} p_i. \tag{2}$$

The mean levels of two classes are described as follows:

$$\mu_0 = \frac{\sum_{i=1}^{t} i p_i}{\omega_0}, \qquad \mu_1 = \frac{\sum_{i=t+1}^{L} i p_i}{\omega_1}. \tag{3}$$

The between-class variance of two classes is defined by (4):

$$f(t) = \sigma_0 + \sigma_1, \tag{4}$$

$$\sigma_0 = \omega_0 (\mu_0 - \mu_T)^2, \qquad \sigma_1 = \omega_1 (\mu_1 - \mu_T)^2, \tag{5}$$

where μ_T is the mean levels of whole image:

$$\mu_T = \sum_{i=1}^{L} i p_i. \tag{6}$$

The optimum threshold t^* is searched exhaustively by maximizing the between-class variance, and the optimal threshold is

$$t^* = \arg\max_{1\leq t\leq L} (f(t)). \tag{7}$$

Otsu's method can be extended to multilevel thresholding. Assume that an image is divided into M classes; the extended between-class variance of m classes is calculated by

$$f(t) = \sum_{i=0}^{M-1} \sigma_i. \tag{8}$$

The sigma terms are determined using (9) and the mean levels are calculated by (10):

$$\begin{aligned} \sigma_0 &= \omega_0 (\mu_0 - \mu_T)^2, \\ \sigma_1 &= \omega_1 (\mu_1 - \mu_T)^2, \\ &\vdots \\ \sigma_{M-1} &= \omega_{M-1} (\mu_{M-1} - \mu_T)^2, \end{aligned} \tag{9}$$

$$\begin{aligned} \mu_0 &= \frac{\sum_{i=1}^{t_1} i p_i}{\omega_0}, \\ \mu_1 &= \frac{\sum_{i=t_1+1}^{t_2} i p_i}{\omega_1}, \\ &\vdots \\ \mu_{M-1} &= \frac{\sum_{i=t_{M-1}+1}^{L} i p_i}{\omega_{M-1}}. \end{aligned} \tag{10}$$

The optimum thresholds are searched by maximizing the between-class variance by

$$t^* = \arg\max_{1\leq t\leq L} \left(\sum_{i=0}^{M-1} \sigma_i \right). \tag{11}$$

2.2. Minimum Cross Entropy Method. Assume that two probability distributions, $p = \{p_1, p_2, \ldots, p_N\}$ and $q = \{q_1, q_2, \ldots, q_N\}$, belong to the same set. The cross entropy between p and q is defined as follows:

$$H(p,q) = \sum_{i=1}^{N} p_i \log \frac{p_i}{q_i}. \tag{12}$$

The concept of cross entropy is widely used for optimization problem, and the minimum cross entropy thresholding method selects an optimal threshold that minimizes the cross entropy between the original image and the processed image. If an original image I in L gray levels can be divided into two segments by threshold t and $f(i)$, where $i = 1, 2, \ldots, L$

is the number of gray levels, then the cross entropy can be calculated by

$$H(t) = \sum_{i=1}^{L} if(i)\log(i) - \sum_{i=1}^{t-1} if(i)\log(\mu(1,t)) - \sum_{i=t}^{L} if(i)\log(\mu(t,L+1)), \tag{13}$$

where

$$\mu(1,t) = \frac{\sum_{i=1}^{t-1} if(i)}{\sum_{i=1}^{t-1} f(i)}, \quad \mu(t,L+1) = \frac{\sum_{i=t}^{L} if(i)}{\sum_{i=t}^{L} f(i)}. \tag{14}$$

We can select an optimal threshold t^* by minimizing the cross entropy based on (13):

$$t^* = \arg\min_{1\le T\le t} \{H(t)\}. \tag{15}$$

Since the first item is constant, the expression of the cross entropy can be modified as

$$\begin{aligned} H(t) &= -\sum_{i=1}^{t-1} if(i)\log(\mu(1,t)) - \sum_{i=t}^{L} if(i)\log(\mu(t,L+1)) \\ &= -m^1(1,t)\log\left(\frac{m^1(1,t)}{m^0(1,t)}\right) - m^1(t,L+1) \\ &\quad \times \log\left(\frac{m^1(t,L+1)}{m^0(t,L+1)}\right), \end{aligned} \tag{16}$$

where $m^0(a,b) = \sum_{i=a}^{b-1} f(i)$ is the zero-moment and $m^1(a,b) = \sum_{i=a}^{b-1} if(i)$ is the first-moment of the image histogram.

It is quite straightforward to extend minimum cross entropy thresholding method to multilevel thresholding segmentation. If an image is required to find M thresholds $(t_1, t_2, \ldots, t_{M-1})$, the cross entropy is given by

$$H(t_1, t_2, \ldots, t_M) = -\sum_{i=1}^{M+1} m^1(t_{i-1}, t_i)\log\left(\frac{m^1(t_{i-1}, t_i)}{m^0(t_{i-1}, t_i)}\right). \tag{17}$$

We can obtain the optimal threshold by minimizing (17). As the swarm intelligence algorithms are usually used to solve maximization problems, we modified (17) as shown below:

$$H(t_1, t_2, \ldots, t_M) = \sum_{i=1}^{M+1} m^1(t_{i-1}, t_i)\log\left(\frac{m^1(t_{i-1}, t_i)}{m^0(t_{i-1}, t_i)}\right). \tag{18}$$

All algorithms used in this paper calculate the minimum cross entropy fitness function by (18) for multilevel thresholding segmentation, which can find the optimal thresholds.

3. Glowworm Swarm Optimization Algorithm

3.1. The Standard Glowworm Swarm Optimization Algorithm. The standard GSO algorithm includes the following steps.

Step 1 (parameters' definition). The key parameters impact the performance of GSO algorithm, that is, s, ρ, β, R_0, and R_s.

Step 2 (glowworms' initialization). In the phase, the glowworms are initially distributed randomly in the given fitness function space so that they are well dispersed, which have equal quantity of luciferin and sensor range. Furthermore, the current iteration is set to 1.

Step 3 (luciferin update phase). The luciferin depends on the function value at the current position of the glowworm, so the position of glowworms changes and the luciferin updates accordingly in the each iteration. Each glowworm updates luciferin according to the following equation:

$$\ell_i(t+1) = (1-\rho)\,\ell_i(t) + \gamma J_i(t+1), \tag{19}$$

where $\ell_i(t)$ is the luciferin of glowworm i at time t, ρ is the luciferin decay constant ($0 < \rho < 1$), γ represents the luciferin enhancement constant, and $J_i(t)$ is the function value.

Step 4 (movement phase). Each glowworm has a variable local-decision domain, which is bounded by a radial sensor range r_s, and is attracted to brighter glowworms. In the movement phase, glowworms search a neighbor by a probabilistic mechanism that has higher luciferin value and move to it. For each glowworm i, the probability equation of moving toward a neighbor j can be stated as

$$p_{ij}(t) = \frac{(\ell_j(t) - \ell_i(t))}{\sum_{k\in N_i(t)} (\ell_k(t) - \ell_i(t))}, \tag{20}$$

where $j \in N_i(t) \ne \Phi$, $N_i(t) = \{j : d_{i,j}(t) < r_d^i(t) \textit{ and } \ell_i(t) < \ell_j(t)\}$ is the set of neighbors of glowworm i, $r_d^i(t)$ is the variable local-decision domain, and $d_{i,j}(t)$ represents the Euclidean distance between glowworms i and j at time t. Then, the equation of the glowworm movements is given by

$$x_i(t+1) = x_i(t) + s\left(\frac{x_j(t) - x_i(t)}{\left\| x_j(t) - x_i(t) \right\|}\right), \tag{21}$$

where $x_i(t)$ represents the location of glowworms i at time t, s is the step size, and $\|\cdot\|$ is the Euclidean norm operator.

Step 5 (local-decision domain update). In the GSO algorithm, the local-decision domain is a dynamic value that is a function with the number of peaks captured. In order to update adaptively the local-decision domain range of each glowworm, the rule is stated as

$$r_d^i(t+1) = \min\left\{r_s, \max\left\{0, r_d^i(t) + \beta\left(n_t - |N_i(t)|\right)\right\}\right\}, \tag{22}$$

where β is a constant parameter and n_t is a threshold parameter used to control the number of neighbors.

```
Set number of dimensions m
Set number of glowworms n
Let x_i(t) be the location of glowworm i at time t
Generate initial population of glowworms x_i (i = 1, 2, ..., n) randomly
for i = 1 to n do ℓ_i(0) = ℓ_0
   r_d^i(0) = r_0;
set maximum iteration number = iter_max
set t = 1
While (t < iter_max) do
{
   s(t) = 3 − (3 − 0.001) * (t/iter_max)^n1
   for each glowworm i do
   ℓ_i(t + 1) = (1 − ρ)ℓ_i(t) + γJ_i(t + 1);
     for each glowworm i do
  {
     N_i(t) = {j : d_i,j(t) < r_d^i(t); ℓ_i(t) < ℓ_j(t)};
       for each glowworm j ∈ N_i(t) do
         p_ij(t) = (ℓ_j(t) − ℓ_i(t))/ ∑_{k∈N_i(t)}(ℓ_k(t) − ℓ_i(t))
     j = select_glowworm (p⃗)
     x_i(t + 1) = x_i(t) + s((x_j(t) − x_i(t))/‖x_j(t) − x_i(t)‖)
     r_d^i(t + 1) = R_S = 255;
     for k = 1 to m do
         x_{i^max,k} ← x_{i^max,k} + α(rand − 0.5);
     end
  }
  t ← t + 1;
}
```

Pseudocode 1: The pseudocode of IGSO algorithm.

3.2. The Proposed Glowworm Swarm Optimization Algorithm. The size step s is a key parameter, which affects the convergence of the GSO algorithm. In GSO algorithm, the step size should be smaller than the ϵ-distance in order to find the optimal solutions [54]. However, the lower step size value may lead to a slow convergence speed. So it can be a large value for starting the algorithm and gradually reducing the value of step size with the increase of iteration [54]. Also, the step size is relevant to the size of the search space. For the larger space, step size must be a larger value. In the standard GSO, s is a constant. In order to improve the convergence of the GSO algorithm, we present a new step size update method in this section. Considering the search space and dimension of image segmentation, the expression is given by

$$s(t) = 3 - (3 - 0.001) * \left(\frac{t}{\text{iter\_max}}\right)^{n1}, \tag{23}$$

where $[0.001, 3]$ is the range of step size, t is iteration, iter_max is the maximum number of iterations, and $n1 = 10^{(-m)}$, where m is the dimension of the search space. When the dimension m is a large value and $n1$ is a low value, the step size will correspondingly increase and algorithm can search more quickly.

The local-decision domain is an important parameter that affects the ability of capturing multiple peaks. When the sensor range of each glowworm extends to the whole search space, all the glowworms move to the global optimal value and ignore the local optimum [54]. To ensure that the GSO algorithm can find the global optimal threshold of image segmentation, the sensor range covers the entire space of image gray histogram $[0, 255]$ and the value is set to 255 in this paper.

In the GSO algorithm, the glowworms with the maximum luciferin remain stationary during the each iteration. The above feature leads to the movements of glowworms that are confined to the interior region of the convex hull [54]. The firefly algorithm can search multiple global solutions simultaneously, and thus it is a very efficient algorithm. However, in the FA algorithm, the brightest fireflies move randomly. So the random movement of the brightest agents is introduced to GSO in this paper.

The pseudocodes of the IGSO algorithm are shown as Pseudocode 1.

4. Results and Discussion

In this paper, the improved glowworm swarm optimization (IGSO) algorithm is applied to the multilevel color image thresholding problem. The RGB color model is a simple and effective model of color image which has three basic color components of red, green, and blue, so we should search the optimal threshold values and fitness values for the each component of the color images. The optimal fitness values (f_{best}) of color image is equal to the sum of the optimal fitness

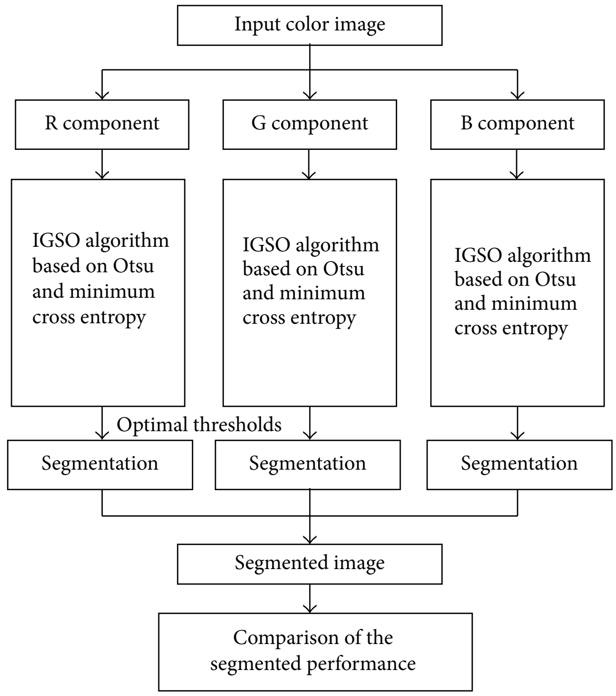

FIGURE 1: The wok of IGSO algorithm for multilevel color image thresholding problem.

values of three components. The work of IGSO algorithm for multilevel color image thresholding problem in this paper is briefly illustrated in Figure 1.

In this section, a large number of experiments are carried out on ten well-known color test images in order to test the performance of the IGSO algorithm for multilevel color image thresholding. Two simple segmentation methods, namely, between-class variance (Otsu) method and minimum cross entropy, are utilized as the fitness functions. All algorithms are implemented in MATLAB Release 2010. Ten well-known color test images and their histograms are shown in Figure 2. All the images are 512×512 in size. The population size is set to be 50 and the maximum number of iterations is 100 in all experiments in this paper. The IGSO algorithm is also compared with two efficient optimization algorithms of APSO and SaDE algorithms. Tables 1–3 give the value of important parameters used for IGSO, APSO, and SaDE algorithms, respectively. In order to estimate the quality of segmented image, the two parameters of peak signal to noise ratio (PSNR) and structural similarity (SSIM) index are used. The higher value of PSNR and SSIM shows a better quality of thresholding.

The peak signal to noise ratio (PSNR) is one of the important performance criteria of image segmentation. The expression of PSNR is defined as follows:

$$\text{PSNR (in dB)} = 20\log_{10}\left(\frac{255}{\text{RMSE}}\right), \tag{24}$$

where

$$\text{RMSE} = \sqrt{\frac{\sum_{I=1}^{M}\sum_{J=1}^{N}\left(I(i,j) - I'(i,j)\right)^2}{MN}}, \tag{25}$$

where $M \times N$ is the size of image, I is the original image, and I' is the segmented image.

TABLE 1: The parameters used in the IGSO algorithm.

Parameters	Explanation	Value
γ	Luciferin enhancement constant	0.6
β	Update rate of decision domain	0.08
ρ	Luciferin decay constant	0.4
R_s	Sensor range	255
$[x_{\min}, x_{\max}]$	Initialization range for the position of the particles	[0, 255]

TABLE 2: The parameters used in the APSO algorithm.

Parameters	Explanation	Value
$w_{\max}$	Maximum of inertia weight	0.9
$w_{\min}$	Minimum of inertia weight	0.1
c_1	Acceleration constants	2.0
c_2	Acceleration constants	2.0
$[x_{\min}, x_{\max}]$	Initialization range for the position of the particles	[0, 255]

(a)

(b)

(c)

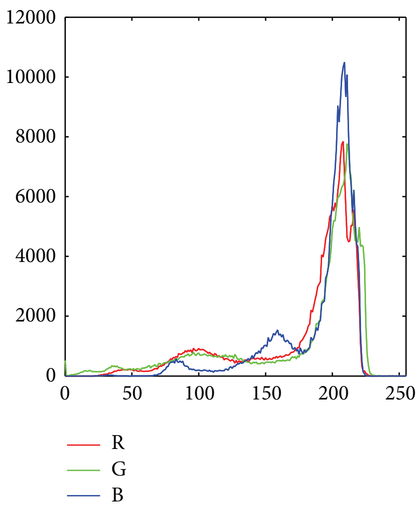

(a′)

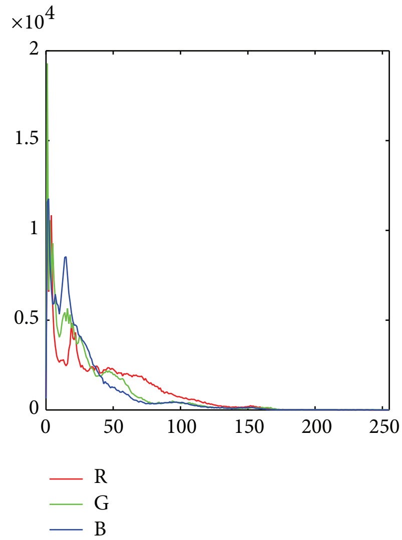

(b′)

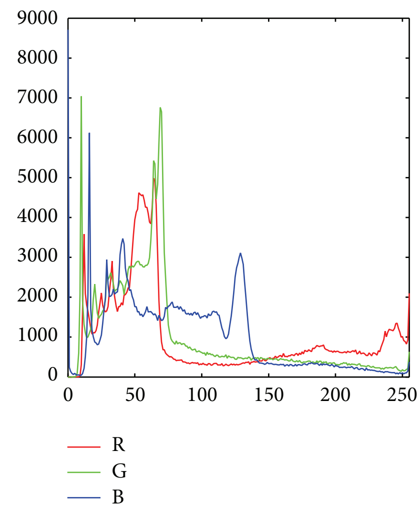

(c′)

(d)

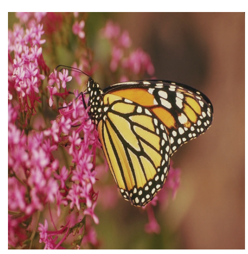

(e)

(f)

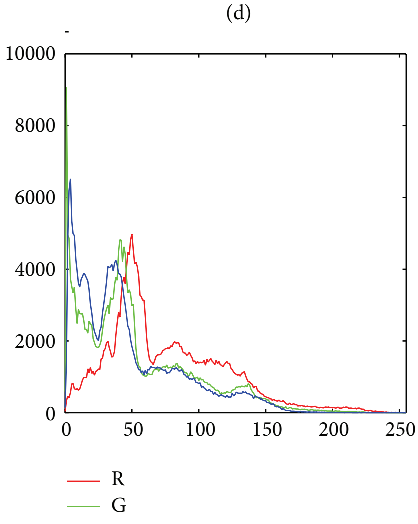

(d′)

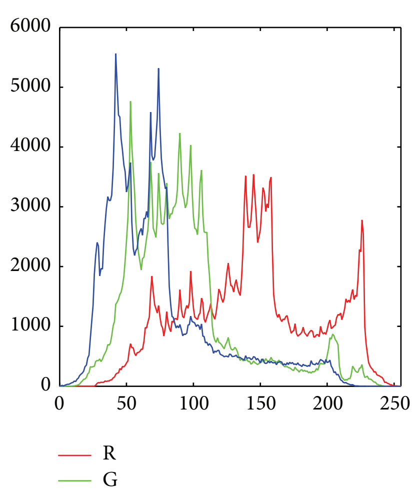

(e′)

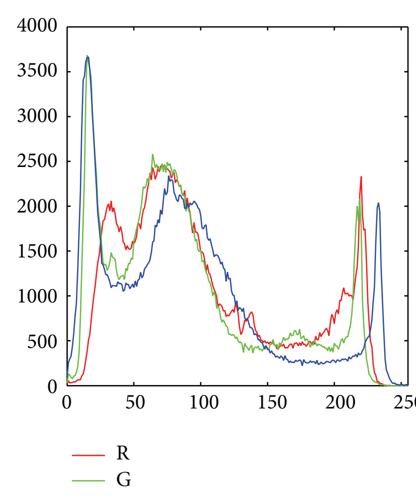

(f′)

Figure 2: Continued.

(g)

(h)

(i)

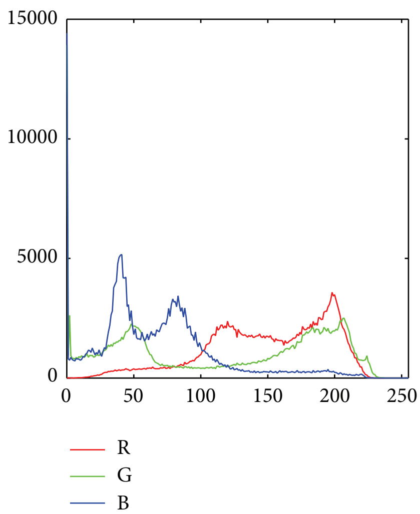

(g′)

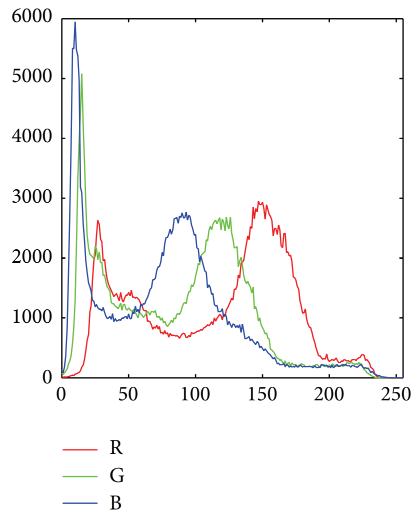

(h′)

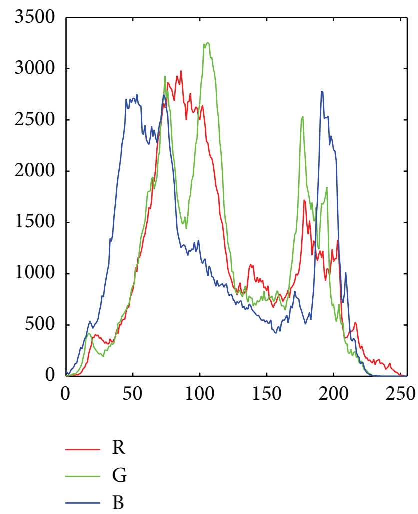

(i′)

(j)

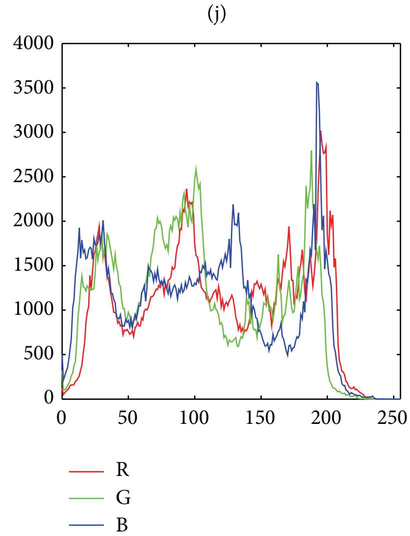

(j′)

Figure 2: The ten test images: (a) airplane, (b) couple, (c) flower, (d) girl, (e) monarch, (f) pen, (g) pepper, (h) soccer, (i) test, and (j) yacht and corresponding histograms: (a′) airplane, (b′) couple, (c′) flower, (d′) girl, (e′) monarch, (f′) pen, (g′) pepper, (h′) soccer, (i′) test, and (j′) yacht.

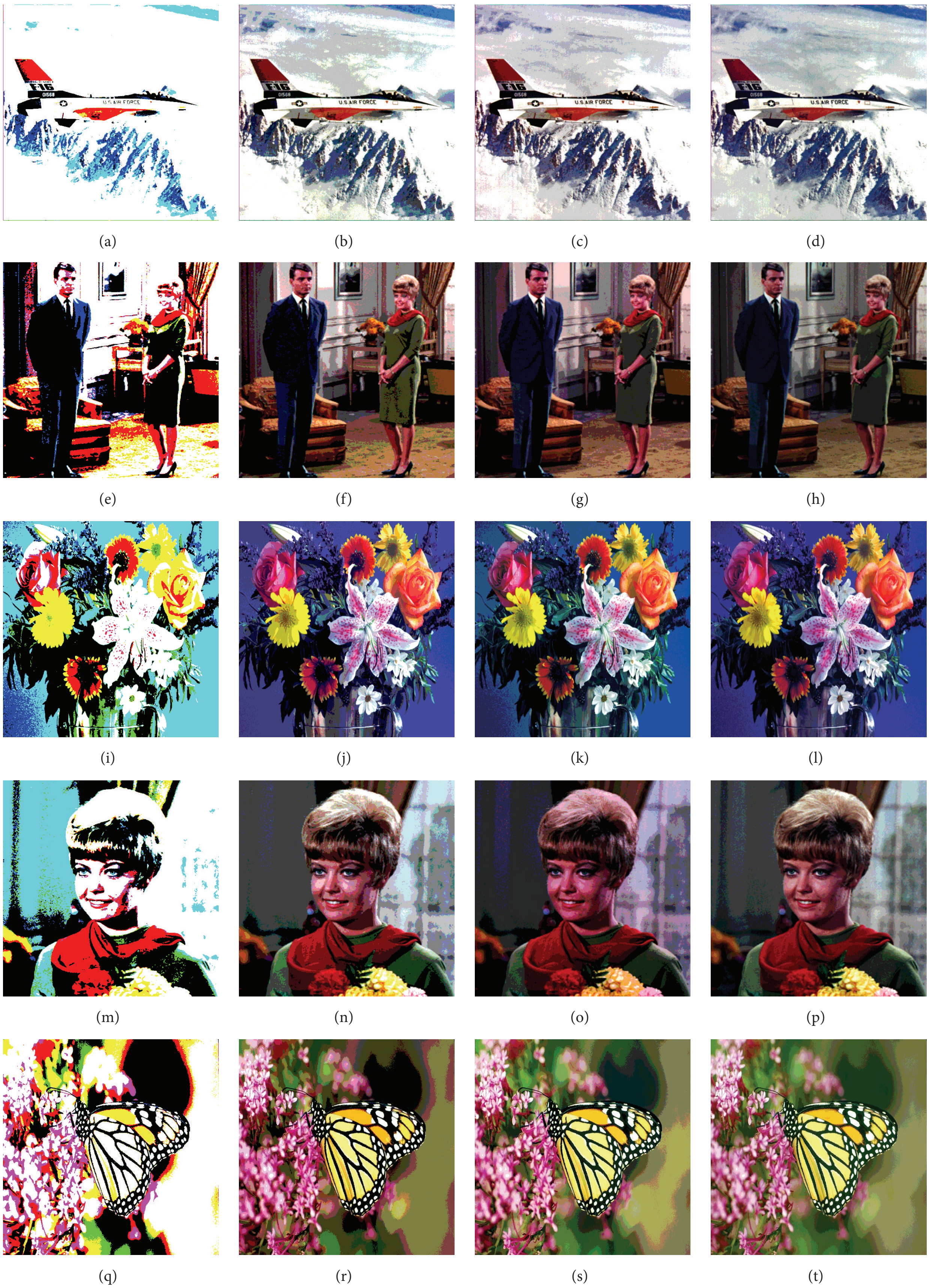

FIGURE 3: For $m = 2$, 4, 6, and 8, images (a)–(d) for airplane, (e)–(h) for couple, (i)–(l) for flower, (m)–(p) for girl, and (q)–(t) for monarch, using IGSO algorithm based on Otsu.

FIGURE 4: For $m = 2$, 4, 6, and 8, images (a)–(d) for pen, (e)–(h) for pepper, (i)–(l) for soccer, (m)–(p) for test, and (q)–(t) for yacht, using IGSO algorithm based on Otsu.

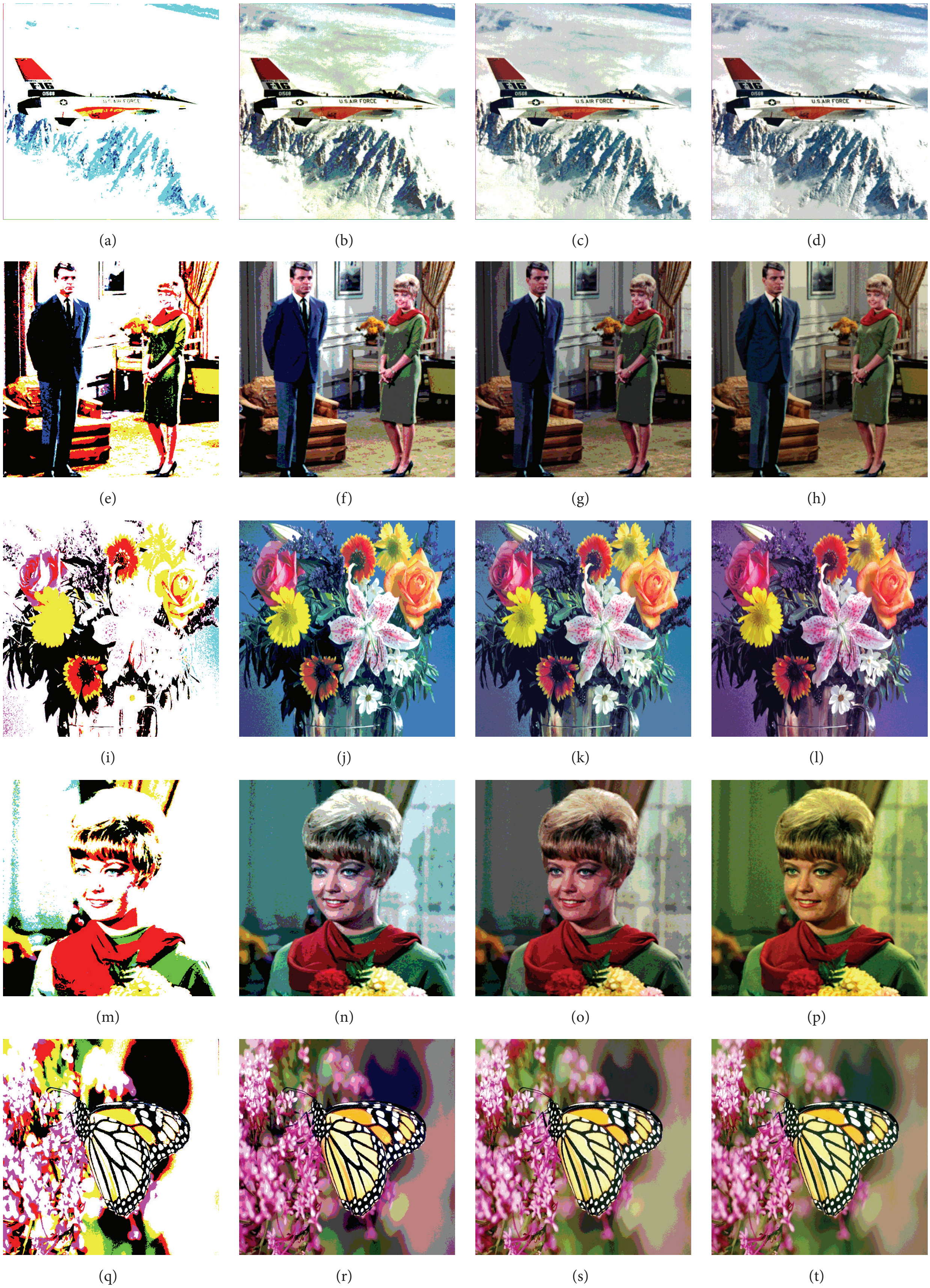

Figure 5: For m =2, 4, 6, and 8, images (a)–(d) for airplane, (e)–(h) for couple, (i)–(l) for flower, (m)–(p) for girl, and (q)–(t) for monarch, using IGSO algorithm based on minimum cross entropy.

FIGURE 6: For $m = 2$, 4, 6, and 8, images (a)–(d) for pen, (e)–(h) for pepper, (i)–(l) for soccer, (m)–(p) for test, and (q)–(t) for yacht, using IGSO algorithm based on minimum cross entropy.

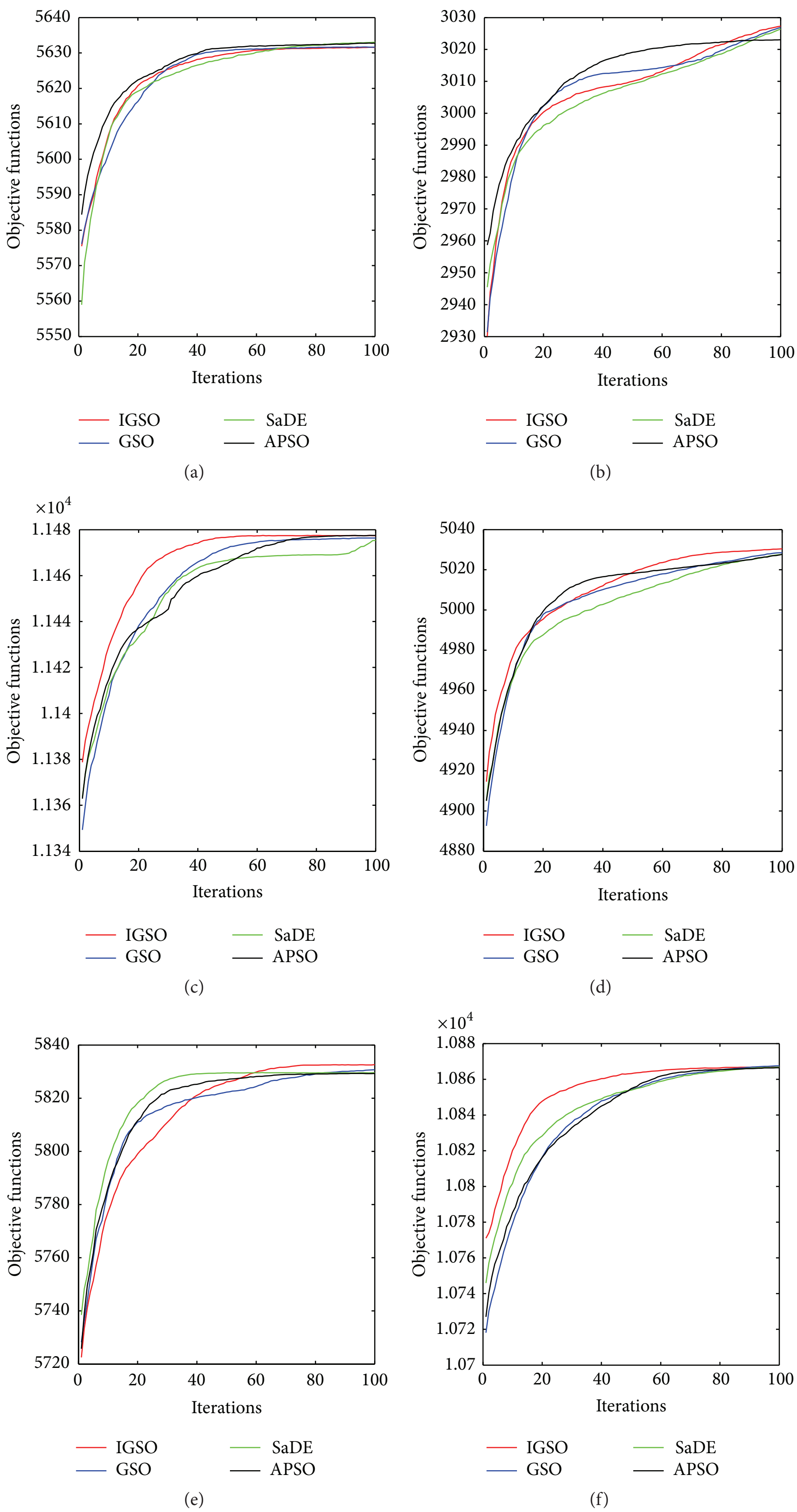

Figure 7: Continued.

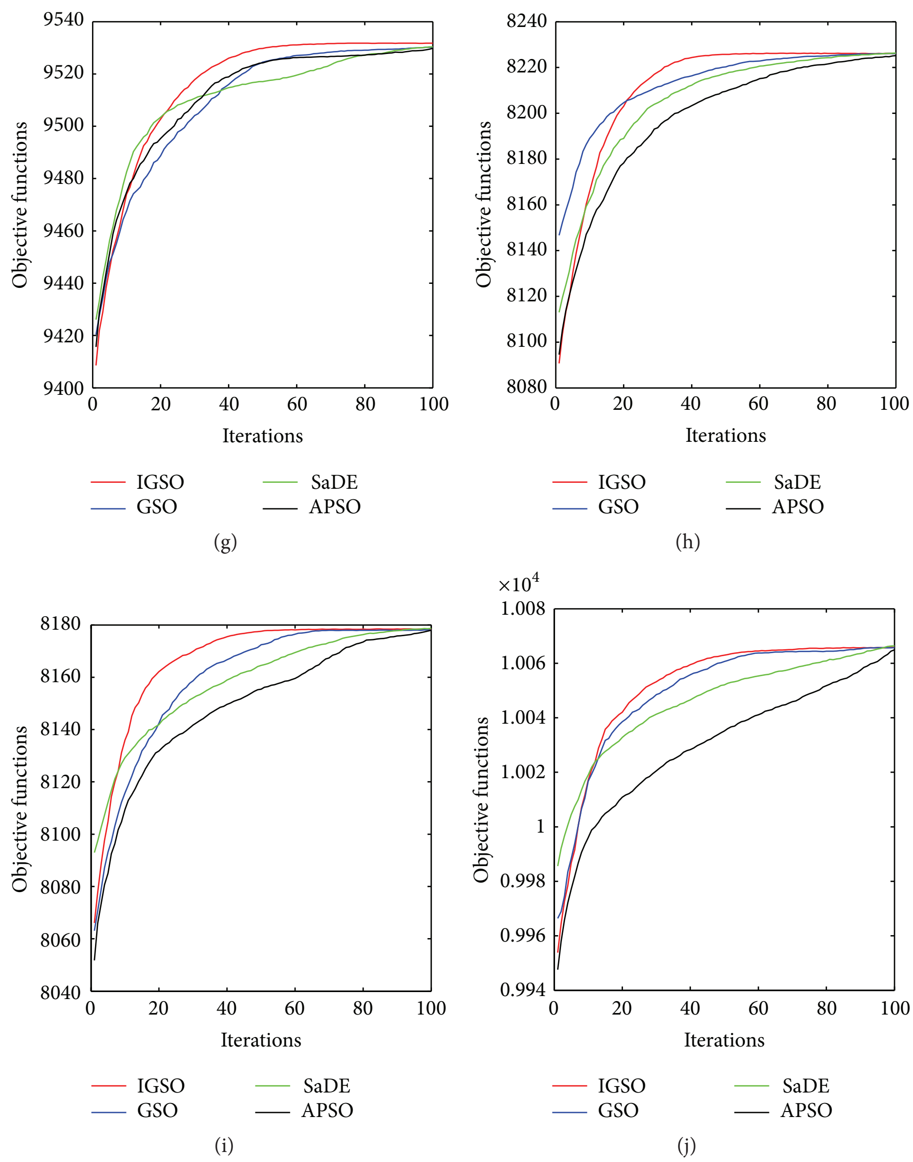

Figure 7: Convergence curves of IGSO, GSO, APSO, and SaDE algorithms for $m = 8$ using Otsu's method.

Table 3: The parameters used in the SaDE algorithm.

Parameters	Explanation	Value
F_0	Differential weight	0.9
CR	Crossover probability	0.1
$[x_{\min}, x_{\max}]$	Initialization range for the position of the particles	[0, 255]

For a RGB color image, the PSNR value of three basic components is computed independently and the average values of them are considered as the PSNR value of color image.

The structural similarity (SSIM) index [55] is used to measure the similarity between the original image and the segmented image. The SSIM between two images can be stated as

$$\mathrm{SSIM}\left(I, I'\right) = \frac{\left(2\mu_I \mu_{I'} + c_1\right)\left(2\sigma_{II'} + c_2\right)}{\left(\mu_I^2 + \mu_{I'}^2 + c_1\right)\left(\sigma_I^2 + \sigma_{I'}^2 + c_2\right)}, \quad (26)$$

where μ_I is the average of I, $\mu_{I'}$ is the average of I', σ_I^2 is the variance of I, $\sigma_{I'}^2$ is the variance of I', $\sigma_{II'}$ is the covariance of I and I', two variables $c_1 = (k_1 L)^2$ and $c_2 = (k_2 L)^2$ stabilize the division with weak denominator, and L is the dynamic range of the pixel-values, $k_1 = 0.01$ and $k_2 = 0.03$. In addition, the SSIM can be extended for color RGB images as shown below:

$$\mathrm{SSIM} = \sum_c \mathrm{SSIM}\left(I^c, I'^c\right), \quad (27)$$

where I^c and I'^c are the cth channel of the original image and segmented color image, respectively, and c is channel number.

Table 4: Optimal thresholds and objective values obtained by IGSO and GSO algorithms using Otsu's method.

m	IGSO R	IGSO G	IGSO B	IGSO f ($\times 10^3$)	GSO R	GSO G	GSO B	GSO f ($\times 10^3$)
				Airplane				
2	120,177	94,166	124,181	5.15456	120,177	94,166	124,181	5.15456
4	83,126,169,199	66,116,164,201	112,150,180,203	5.48484	83,126,169,199	66,116,164,201	112,150,180,203	5.48484
6	68,99,129,162,187,204	57,98,132,167,193,209	102,134,156,176,195,207	**5.58695**	68,100,130,162,187,204	55,98,133,167,193,207	102,136,156,176,196,209	5.58690
8	64,92,114,140,163,184,198,209	47,80,107,132,159, 183,200,212	56,102,132,152,170,188,201,211	**5.63154**	63,93,116,141,166,186,199,210	47,81,108,134,161,184,202,214	57,104,134,154,173,190,202,211	5.63124
				Couple				
2	35,83	30,81	27,76	2.64122	35,83	30,81	27,76	2.64122
4	17,42,71,109	16,39,74,122	17,39,72,117	2.91159	17,42,71,109	16,39,74,122	17,39,72,117	2.91159
6	13,32,52,73,97,131	13,31,51,81,123,176	11,26,46,77,119,177	**2.99013**	15,33,52,75,97,131	13,32,54,81,123,176	13,27,46,77,119,178	2.99009
8	12,28,45,62,81,104,135,204	10,23,37,54,78,104,138,200	9,22,38,56,80,108,142,180	**3.02731**	12,29,43,61,78,100,131,200	10,24,40,60,73,86,106,135,201	9.20,34,55,74,102,133,176	3.02709
				Flower				
2	101,190	53,129	73,151	10.35564	101,190	53,129	73,151	10.35564
4	42,92,154,209	44,84,132,188	32,68,108,163	11.25529	42,92,154,209	44,84,132,188	32,68,108,163	11.25529
6	41,76,119,160,194,226	32,56,84,121,162,206	26,55,86,114,152,199	**11.38993**	41,76,118,159,193,225	32,54,82, 121,163,206	26,55,83,114,152,198	11.38990
8	35,53,78,109,142,173,201,229	30,54,77,102,129,157,189,222	20,38,55,76,96,118,154,200	**11.47485**	34,53,76,109,142,172,200,228	31,54,77,101,138,162,193,220	24,40,59,72,91,117,161,209	11.47454
				Girl				
2	69,124	34,88	31,81	4.34647	69,124	34,88	31,81	4.34647
4	37,69,106,155	25,58,92,129	24,52,81,117	4.84594	37,69,106,155	25,58,92,129	24,52,81,117	4.84594
6	35,62,88,112,140,179	25,57,89,124,194,208	23,44,67,94,124,190	**4.93170**	34,62,89,114,140,179	22,57,89,123,194,208	23,48,67,94,124,190	4.93167
8	27,44,64,83,104,125,151,187	16,34,52,72,92,115,138,169	13,29,47,67,88,110,134,163	**5.02842**	26,45,65,87,112,130,160,192	12,31,50,67,88,110,136,172	12,25,40,65,84,103,131,167	5.02814
				Monarch				
2	114,176	79,142	62,122	5.19253	114,176	79,142	62,122	5.19253
4	89,127,162,198	63,90,125,175	55,86,122,164	5.63990	89,127,162,198	63,90,125,175	55,86,122,164	5.63990
6	77,105,129,149,174,204	45,64,83,103,134,180	40,60,85,113,144,177	**5.77439**	79,105,129,150,174,206	48,64,83,104,134,181	40,60,85,113,141,178	5.77434
8	63,85,109,130,148,166,191,212	12,45,63,81,98,119,149,186	38,54,70,86,108,131,156,184	**5.83061**	68,90,103,123,145,160,187,208	21,46,63,81,98,119,149,186	35,49,63,80,101,127,149,182	5.83002
				Pen				
2	76,151	60,138	63,152	9.77709	76,151	60,138	63,152	9.77709
4	51,84,124,178	44,82,128,183	44,85,125,184	10.58262	51,84,124,178	44,82,128,183	44,85,125,184	10.58262
6	44,69,92,120,157,195	36,63,86,114,151,192	32,61,88,115,153,201	**10.78635**	44,69,93,120,156,194	36,63,85,114,152,192	32,61,88,117,155,201	10.78632
8	39,59,77,96,120,149,179,206	29,50,70,89,110,137,169,199	29,53,74,93,116,142,177,212	**10.86604**	36,55,74,93,114,141,171,202	28,48,67,85,106,145,176,199	27,49,70,90,110,135,169,209	10.86570
				Pepper				
2	97,159	78,157	58,127	8.61756	97,159	78,157	58,127	8.61756
4	81,124,156,186	30,82,140,185	25,60,95,146	9.28037	81,124,156,186	30,82,140,185	25,60,95,146	9.28037
6	62,96,121,143,167,191	20,46,81,125,163,193	23,50,73,96,129,172	**9.45358**	64,97,122,143,168,191	20,49,81,126,163,194	20,50,73,96,129,171	9.45354
8	53,85,107,127,145,164,183,199	17,42,69,100,132,159,182,201	11,32,50,69,87,108,140,177	**9.53018**	54,85,108,128,145,165,184,200	17,40,64,92,122,153,177,199	11,31,50,69,87,108,140,179	9.52962
				Soccer				
2	86,149	71,138	55,126	7.27688	86,149	71,138	55,126	7.27688
4	57,103,144,180	41,83,120,166	38,77,113,166	7.96150	57,103,144,180	41,83,120,166	38,77,113,166	7.96150
6	44,75,109,137,160,192	30,57,86,112,135,175	27,56,82,105,133,177	**8.15225**	44,75,108,136,159,192	32,58,87,113,136,176	27,55,82,105,133,179	8.15218
8	40,63,86,113,135,153,171,198	26,48,73,97,114,133,158,192	23,46,68,86,105,127,154,192	**8.22619**	36,58,79,110,129,147,168,195	24,43,69,95,111,129,151,186	22,45,67,86,104,126,155,192	8.22581
				Test				
2	89,148	86,144	82,150	7.43581	89,148	86,144	82,150	7.43581
4	61,92,127,171	57,90,126,165	55,88,127,172	7.94367	61,92,127,171	57,90,126,165	55,88,127,172	7.94367
6	52,78,100,127,161,193	46,72,95,124,157,185	40,62,86,114,147,181	**8.10926**	51,77,100,127,160,194	45,71,95,124,158,185	40,62,86,1154,147,182	8.10922
8	45,68,87,104,129,157,184,207	43,67,88,107,130,158,180,198	33,52,69,90,115,145,176,197	**8.17834**	40,63,78,99,124,147,175,204	36,59,85,102,126,153,172,196	35,51,67,86,106,138,173,189	8.17792
				Yacht				
2	71,141	64,132	74,148	9.16339	71,141	64,132	74,148	9.16339
4	56,97,136,176	50,86,125,166	45,85,120,163	9.83344	56,97,136,176	50,86,125,166	45,85,120,163	9.83344
6	46,78,105,133,160,185	48,81,111,141,168,189	28,55,86,115,144,176	**9.98335**	45,78,105,132,159,185	48,80,109,140,168,189	29,55,86,115,143,176	9.98330
8	37,62,84,107,132,155,173,190	29,53,74,92,110,133,155,178	25,49,74,97,118,139,162,185	**10.00658**	32,59,75,105,130, 146,162,185	29,51,74,92,110,133,156,179	24,48,70,91,112,132,154,181	10.00622

Table 5: Optimal thresholds and objective values obtained by APSO and SaDE algorithms using Otsu's method.

m	APSO R	APSO G	APSO B	APSO f ($\times 10^3$)	SaDE R	SaDE G	SaDE B	SaDE f ($\times 10^3$)
				Airplane				
2	120,177	94,166	124,181	5.15456	120,177	94,166	124,181	5.15456
4	83,126,169,199	66,116,164,201	112,150,180,203	5.48484	83,126,169,199	66,116,164,201	112,150,180,203	5.48484
6	71,102,130,164,190,204	59,99,134,169,194,211	104,136,157,179,196,207	5.58678	69,101,131,163,188,204	57,100,133,167,192,210	102,135,158,177,196,203	5.58683
8	63,90,110,134,160,180,197,209	45,79,105,129,154,180,199,207	52,97,125,150,168,186,200,210	5.63107	64,91,111,136,161,182,197,209	46,79,105,130,156,181,198,208	53,99,127,150,169,188,201,210	5.63113
				Couple				
2	35,83	30,81	27,76	2.64122	35,83	30,81	27,76	2.64122
4	17,42,71,109	16,39,74,122	17,39,72,117	2.91159	17,42,71,109	16,39,74,122	17,39,72,117	2.91159
6	16,34,52,76,99,136	15,32,56,84,126,179	13,32,48,78,122,178	2.98998	14,33,53,75,98,133	14,33,55,82,127,177	14,27,46,79,121,179	2.99003
8	13,30,48,67,87,110,142,205	10,24,40,56,82,113,149,206	10,24,41,64,90,122,146,187	3.02679	13,30,48,66,85,109,139,204	10,23,39,55,83,109,143,202	11,23,40,62,88,119,147,185	3.02687
				Flower				
2	101,190	53,129	73,151	10.35564	101,190	53,129	73,151	10.35564
4	42,92,154,209	44,84,132,188	32,68,108,163	11.25529	42,92,154,209	44,84,132,188	32,68,108,163	11.25529
6	42,77,123,163,196,224	35,59,90,122,165,208	26,57,86,116,156,197	11.38983	41,74,117,159,191,225	34,56,86,123,159,203	27,55,84,112,150,200	11.38986
8	34,54,79,115,149,176,203,230	32,55,81,110,139,167,192,225	24,44,63,81,100,121,155,202	11.47416	35,54,78,112,146,176,202,230	31,54,78,106,137,158,192,226	22,43,60,81,100,120,153,201	11.47424
				Girl				
2	69,124	34,88	31,81	4.34647	69,124	34,88	31,81	4.34647
4	37,69,106,155	25,58,92,129	24,52,81,117	4.84594	37,69,106,155	25,58,92,129	24,52,81,117	4.84594
6	37,60,85,108,138,178	28,59,93,125,196,210	27,45,69,96,127,195	4.93159	35,65,89,113,141,179	24,59,90,127,196,209	26,46,69,95,126,192	4.93162
8	29,47,67,89,110,131,155,190	17,36,58,81,102,123,130,164	16,34,51,73,92,116,139,167	5.02802	27,46,66,87,107,127,156,192	17,35,55,74,95,119,139,175	15,32,50,71,91,114,137,165	5.02796
				Monarch				
2	114,176	79,142	62,122	5.19253	114,176	79,142	62,122	5.19253
4	89,127,162,198	63,90,125,175	55,86,122,164	5.63990	89,127,162,198	63,90,125,175	55,86,122,164	5.63990
6	78,109,133,151,176,205	46,66,84,105,137,183	42,61,87,116,146,180	5.77425	79,104,130,153,175,205	46,62,82,101,132,179	40,62,87,114,145,178	5.77428
8	62,82,104,123,144,162,189,217	13,49,67,88,100,123,158,192	38,55,70,90,116,141,166,186	5.82961	62,84,105,125,145,164,187,210	17,46,68,84,101,121,153,191	39,56,73,93,105,135,160,184	5.82970
				Pen				
2	76,151	60,138	63,152	9.77709	76,151	60,138	63,152	9.77709
4	51,84,124,178	44,82,128,183	44,85,125,184	10.58262	51,84,124,178	44,82,128,183	44,85,125,184	10.58262
6	46,72,94,121,158,196	38,66,89,116,153,193	35,62,91,117,152,199	10.78625	44,71,91,122,158,197	37,64,87,116,153,192	33,63,88,116,153,199	10.78627
8	42,64,82,104,126,158,185,209	30,53,74,95,120,151,177,202	29,55,79,100,122,151,183,215	10.86558	40,62,81,101,126,154,184,208	30,50,71,92,116,145,174,201	30,55,78,98,122,148,182,214	10.86549
				Pepper				
2	97,159	78,157	58,127	8.61756	97,159	78,157	58,127	8.61756
4	81,124,156,186	30,82,140,185	25,60,95,146	9.28037	81,124,156,186	30,82,140,185	25,60,95,146	9.28037
6	61,91,120,141,168,191	22,47,84,127,166,194	22,48,69,94,128,171	9.45348	59,93,121,142,167,191	24,48,81,126,164,193	20,49,72,96,130,172	9.45350
8	49,77,102,122,141,162,183,198	19,45,71,107,138,165,185,203	13,32,54,74,89,114,147,184	9.52933	53,79,104,124,143,161,179,198	20,42,71,105,137,162,187,202	12,35,51,71,90,111,145,183	9.52941
				Soccer				
2	86,149	71,138	55,126	7.27688	86,149	71,138	55,126	7.27688
4	57,103,144,180	41,83,120,166	38,77,113,166	7.96150	57,103,144,180	41,83,120,166	38,77,113,166	7.96150
6	44,78,110,139,158,193	32,60,87,112,136,175	30,59,84,106,133,178	8.15211	45,76,111,137,159,192	31,59,88,114,136,176	28,58,84,107,134,178	8.15213
8	46,68,90,119,137,158,176,199	28,51,75,102,118,136,163,199	27,51,70,91,110,134,162,202	8.22550	40,65,92,118,138,155,174,200	27,50,76,98,116,136,165,195	25,48,71,89,109,133,163,198	8.22559
				Test				
2	89,148	86,144	82,150	7.43581	89,148	86,144	82,150	7.43581
4	61,92,127,171	57,90,126,165	55,88,127,172	7.94367	61,92,127,171	57,90,126,165	55,88,127,172	7.94367
6	51,79,102,129,160,194	48,73,96,127,158,185	39,60,83,114,145,180	8.10924	51,76,99,126,159,193	45,71,95,123,159,186	41,63,86,113,149,182	8.10927
8	48,70,91,110,137,164,185,210	41,72,89,112,132,165,186,203	39,56,77,98,120,154,176,202	8.17762	47,71,89,109,133,161,187,209	43,69,91,109,133,163,184,201	37,57,75,96,121,150,177,197	8.17770
				Yacht				
2	71,141	64,132	74,148	9.16339	71,141	64,132	74,148	9.16339
4	56,97,136,176	50,86,125,166	45,85,120,163	9.83344	56,97,136,176	50,86,125,166	45,85,120,163	9.83344
6	46,76,103,132,160,183	49,84,114,141,169,189	29,57,85,114,142,176	9.98324	45,77,105,132,159,185	47,80,110,139,168,190	27,56,86,116,145,175	9.98326
8	42,65,90,112,134,163.181,198	26,45,66,83,101,126,151,175	25,49,70,95,109,142,165,189	10.00592	41,66,87,111,135,160,178,195	25,49,68,86,103,128,150,177	27,51,758,98,120,141,166,188	10.00601

Table 6: Comparison of optimal PSNR (dB) and SSIM values obtained by IGSO, GSO, APSO, and SaDE algorithms using Otsu's method.

Image	m	IGSO		GSO		APSO		SaDE	
		PSNR	SSIM	PSNR	SSIM	PSNR	SSIM	PSNR	SSIM
Airplane	2	10.0144	0.7740	10.0144	0.7740	10.0144	0.7740	10.0144	0.7740
	4	10.0188	0.8246	10.0188	0.8246	10.0188	0.8246	10.0188	0.8246
	6	10.0300	0.8575	10.0263	0.8398	10.0211	0.8346	10.0243	0.8369
	8	**10.3589**	**0.9134**	10.3524	0.9029	10.3439	0.8958	10.3481	0.9016
Couple	2	**27.0382**	**0.8025**	27.0382	0.8025	27.0382	0.8025	27.0382	0.8025
	4	27.0470	0.8830	27.0470	0.8830	27.0470	0.8830	27.0470	0.8830
	6	**27.0579**	**0.9143**	27.0518	0.9093	27.0492	0.8976	27.0507	0.9036
	8	**27.0602**	**0.9427**	27.0559	0.9362	27.0517	0.9294	27.0526	0.9316
Flower	2	19.3175	0.8460	19.3175	0.8460	19.3175	0.8460	19.3175	0.8460
	4	19.3280	0.9040	19.3280	0.9040	19.3280	0.9040	19.3280	0.9040
	6	**19.3296**	**0.9372**	19.3278	0.9340	19.3283	0.9207	19.3289	0.9222
	8	**20.3152**	**0.9604**	20.2937	0.9549	20.2859	0.9508	20.2924	0.9526
Girl	2	24.0610	0.7112	24.0610	0.7112	24.0610	0.7112	24.0610	0.7112
	4	24.0734	0.8011	24.0734	0.8011	24.0734	0.8011	24.0734	0.8011
	6	**24.0798**	**0.8584**	24.0766	0.8546	24.0739	0.8512	24.0748	0.8527
	8	**24.0824**	**0.9094**	24.0802	0.8982	24.0767	0.8927	24.0789	0.8936
Monarch	2	19.4727	0.7658	19.4727	0.7658	19.4727	0.7658	19.4727	0.7658
	4	19.4767	0.8589	19.4767	0.8589	19.4767	0.8589	19.4767	0.8589
	6	**19.4785**	**0.9155**	19.4778	0.9116	19.4771	0.9059	19.4776	0.9081
	8	**19.4941**	**0.9454**	19.4879	0.9387	19.4811	0.9255	19.4918	0.9312
Pen	2	19.8912	0.8420	19.8912	0.8420	19.8912	0.8420	19.8912	0.8420
	4	19.8935	0.8791	19.8935	0.8791	19.8935	0.8791	19.8935	0.8791
	6	19.8983	0.9330	19.8961	0.9238	19.8938	0.9170	19.8947	0.9215
	8	19.9014	0.9629	19.9001	0.9581	19.8979	0.9543	19.8990	0.9566
Pepper	2	18.1771	0.8046	18.1771	0.8046	18.1771	0.8046	18.1771	0.8046
	4	18.1789	0.8384	18.1789	0.8384	18.1789	0.8384	18.1789	0.8384
	6	**18.1856**	**0.9004**	18.1825	0.8976	18.1796	0.8880	18.1811	0.8916
	8	**18.1891**	**0.9476**	18.1836	0.9302	18.1801	0.9164	18.1822	0.9251
Soccer	2	20.3329	0.8088	20.3329	0.8088	20.3329	0.8088	20.3329	0.8088
	4	20.3368	0.8570	20.3368	0.8570	20.3368	0.8570	20.3368	0.8570
	6	**20.3466**	**0.9023**	20.3421	0.8931	20.3389	0.8822	20.3405	0.8886
	8	**20.3474**	**0.9529**	20.3437	0.9493	20.3410	0.9330	20.3422	0.9375
Test	2	18.5023	0.7611	18.5023	0.7611	18.5023	0.7611	18.5023	0.7611
	4	18.5081	0.8508	18.5081	0.8508	18.5081	0.8508	18.5081	0.8508
	6	**18.5106**	**0.9017**	18.5091	0.8959	18.5086	0.8883	18.5089	0.8913
	8	**18.5144**	**0.9446**	18.5120	0.9274	18.5095	0.9122	18.5107	0.9208
Yacht	2	18.5073	0.8133	18.5073	0.8133	18.5073	0.8133	18.5073	0.8133
	4	18.5083	0.8503	18.5083	0.8503	18.5083	0.8503	18.5083	0.8503
	6	**18.5090**	**0.9035**	18.5086	0.8910	18.5082	0.8865	18.5085	0.8894
	8	**18.5164**	**0.9542**	18.5122	0.9389	18.5097	0.9120	18.5106	0.9274

4.1. Experiment 1. In this section, the IGSO algorithm is used for ten color test images using Otsu's method as fitness function and the results are compared with the GSO, APSO, and SaDE algorithms. Tables 4 and 5 present the number of thresholds (m), corresponding optimal thresholds, and objective values for $m = 2, 4, 6$, and 8 computed by IGSO, APSO, and SaDE algorithms using Otsu's method. In Table 6, comparison of PSNR (dB) and SSIM values is depicted for each method and number of thresholds, which reveals the quality of segmented images. The segmented images using IGSO algorithm based on Otsu's method at 2, 4, 6, and 8 levels of thresholding are shown in Figures 3 and 4.

4.2. Experiment 2. In the second part of the experiments, we find optimal threshold values by maximizing the modified equation (18). The number of thresholds, the optimal thresholds, and the optimal objective values for IGSO, GSO, APSO, and SaDE algorithms are listed in Tables 7 and 8.

Table 7: Optimal thresholds and objective values obtained by IGSO and GSO algorithms using MCE.

m	IGSO R	IGSO G	IGSO B	IGSO f ($\times 10^2$)	GSO R	GSO G	GSO B	GSO f ($\times 10^2$)
				Airplane				
2	109,168	72,153	120,180	28.75021	109,168	72,153	120,180	28.75021
4	73,117,162,197	53,100,146,191	109,147,178,203	28.7628	73,117,162,197	53,100,146,191	109,147,178,203	28.7628
6	65,95,124,155,183,204	28,63,100,136,177,205	57,108,144,169,191,207	**28.76704**	64,95,124,155,183,203	29,63,100,136,176,205	56,107,143,169,190,207	28.76703
8	59,85,105,127,152,176,194,207	24,53,82,108,137,168,193,210	55,96,121,146,163,181,198,208	**28.76901**	59,85,105,128,153, 176,194,208	24,53,81,108,136,167,192,209	52,95,121,145,163,181,198,209	28.76899
				Couple				
2	26,78	21,74	22,71	3.97893	26,78	21,74	22,71	3.97893
4	12,30,57,93	8,22,42,81	8,21,40,78	4.02494	12,30,57,93	8,22,42,81	8,21,40,78	4.02494
6	10,29,52,82,126,209	9,22,40,68,111,232	7,21,39,72,137,192	**4.02990**	10,30,53,84,134,210	7,21,39,71,115,235	8,21,40,74,145,196	4.02989
8	6,15,28,44,62,85,118,178	4,11,20,35,52,78,120,232	6,13,26,41,69,109,176,218	**4.03718**	6,15,28,45,64,87,120,183	5,11,21,35,52,80,122,223	5,12,22,39,67,108,173,217	4.03715
				Flower				
2	41,119	44,111	53,114	12.34354	41,119	44,111	53,114	12.34354
4	39,79,135,199	27,52,93,159	23,56,98,157	12.39484	39,79,135,199	27,52,93,159	23,56,98,157	12.39484
6	26,47,75,118,166,213	22,40,59,85,129,184	6,34,63,99,142,189	**12.40942**	26,48,75,118,167,213	22,40,60,86,128,184	8,33,62,99,141,190	12.40941
8	20,32,46,59,83,125,171,215	21,38,57,79,105,134,171,210	7,28,45,66,89,115,150,197	**12.41612**	23,35,48,62,84,127,172,216	21,39,53,76,102,133,171,212	6,27,47,67,90,115,153,203	12.41609
				Girl				
2	41,90	22,72	26,80	7.65874	41,90	22,72	26,80	7.65874
4	33,65,102,149	11,31,62,109	11,28,56,101	7.70152	33,65,102,149	11,31,62,109	11,28,56,101	7.70152
6	23,43,66,96,131,185	10,29,56,86,122,181	12,28,55,96,145,167	**7.70996**	22,43,66,98,132,186	10,30,58,87,123,182	11,27,55,95,145,167	7.70995
8	17,34,48,65,85,107,130,169	5,14,27,40,59,84,113,149	16,47,53,132,146,171,207,242	**7.71557**	19,38,50,67,87,110,133,168	7,16,30,42,62,88,114,156	13,45,52,131,147,168,205,239	7.71555
				Monarch				
2	108,172	75,135	58,113	14.98290	108,172	75,135	58,113	14.98290
4	79,115,147,186	61,86,119,169	38,61,91,141	15.00562	79,115,147,186	61,86,119,169	38,61,91,141	15.00562
6	62,85,110,137,165,200	44,63,81,100,130,177	36,50,66,88,119,162	**15.01305**	62,85,111,137,165,198	45,63,81,102,130,177	35,50,67,89,121,163	15.01304
8	59,79,97,115,134,151,175,204	36,49,64,80,96,117,146,185	33,45,57,71,88,112,140,173	**15.01603**	62,83,100,117,137,153,178,206	33,47,61,78,95,115,143,182	35,49,60,71,86,111,141,174	15.01600
				Pen				
2	61,133	48,125	49,136	13.20604	61,133	48,125	49,136	13.20604
4	45,76,112,169	34,66,101,157	29,63,102,166	13.25261	45,76,112,169	34,66,101,157	29,63,102,166	13.25261
6	35,56,79,106,143,187	26,47,70,95,133,183	22,44,69,95,128,182	**13.26480**	34,56,79,106,142,188	26,47,70,95,134,183	22,43,69,95,128,183	13.26479
8	30,46,63,80,100,127,161,199	22,38,56,73,92,117,151,191	16,29,48,69,90,113,148,198	**13.27007**	30,47,67,85,103,131,162,201	24,41,60,78,93,121,155,204	17,33,52,70,93,115,151,200	13.27003
				Pepper				
2	87,153	22,104	21,74	16.40133	87,153	22,104	21,74	16.40133
4	62,102,137,174	10,39,85,156	15,52,83,133	16.45113	62,102,137,174	10,39,85,156	15,52,83,133	16.45113
6	51,84,111,135,162,189	8,33,63,102,149,188	7,29,54,80,116,170	**16.46417**	52,82,111,135,162,188	8,33,62,102,148,187	6,28,55,81,117,172	16.46416
8	44,69,94,115,133,153,174,194	6,23,42,65,97,134,167,195	6,26,47,67,89,115,151,189	**16.46928**	44,70,95,116,134,154,175,195	6,27,45,68,94,120,170,197	6,23,42,67,93,118,153,192	16.46926
				Soccer				
2	64,126	42,97	42,113	13.11371	64,126	42,97	42,113	13.11371
4	43,79,123,165	30,63,105,155	25,60,99,150	13.15363	43,79,123,165	30,63,105,155	25,60,99,150	13.15363
6	37,61,92,126,155,188	22,41,67,96,124,167	20,45,75,103,140,191	**13.16536**	38,62,92,127,155,188	22,42,67,96,126,166	20,46,75,105,142,194	13.16535
8	32,48,68,93,120,143,163,193	21,36,55,77,99,118,138,175	13,24,41,62,84,103,128,171	**13.17071**	32,48,68,94,121,144,164,194	21,37,59,80,101,120,139,178	16,30,43,60,79,103,125,174	13.17068
				Test				
2	80,137	83,140	67,132	16.22951	80,137	83,140	67,132	16.22951
4	55,88,122,167	40,70,97,143	39,65,100,155	16.25759	55,88,122,167	40,70,97,143	39,65,100,155	16.25759
6	43,70,93,121,156,190	37,64,90,116,149,182	29,48,68,91,125,169	**16.26698**	43,70,94,120,155,190	38,66,91,118,150,182	31,49,67,92,126,169	16.26697
8	36,58,74,92,108,131,162,194	31,53,70,88,107,129,159,186	27,45,61,79,99,125,154,183	**16.27108**	37,59,76,93,110,134,163,196	31,55,72,92,111,134,163,187	27,43,58,74,95,121,152,181	16.27105
				Yacht				
2	60,133	55,125	53,127	15.87338	60,133	55,125	53,127	15.87338
4	44,80,119,166	28,56,92,139	25,55,99,154	15.91058	44,80,119,166	28,56,92,139	25,55,99,154	15.91058
6	30,53,80,108,140,177	24,48,73,96,127,168	21,40,65,92,123,162	**15.92188**	30,52,80,107,140,177	25,47,73,96,127,167	20,40,65,91,121,162	15.92187
8	25,41,62,84,107,133,159,185	21,36,55,76,95,118,146,174	16,29,48,70,93,118,144,175	**15.92650**	25,45,63,84,108,130,154,187	21,39,58,82,96,119,147,174	16,30,49,73,95,122,144,177	15.92647

Table 8: Optimal thresholds and objective values obtained by APSO and SaDE algorithms using MCE.

m	APSO				SaDE			
	R	G	B	f ($\times 10^2$)	R	G	B	f ($\times 10^2$)
				Airplane				
2	109,168	72,153	120,180	28.75021	109,168	72,153	120,180	28.75021
4	73,117,162,197	53,100,146,191	109,147,178,203	28.7628	73,117,162,197	53,100,146,191	109,147,178,203	28.7628
6	63,95,123,156,185,205	28,65,102,137,177,208	54,109,144,169,193,209	28.76701	64,95,123,155,183,203	29,64,100,136,176,203	58,107,143,169,190,206	28.76702
8	58,82,101,123,147,172,192,206	26,57,87,111,139,171,194,209	48,94,120,144,162,180,197,208	28.76895	59,84,103,126,149,174,193,205	24,53,85,110,139,170,194,210	53,95,119,145,161,180,198,209	28.76897
				Couple				
2	26,78	21,74	22,71	3.97893	26,78	21,74	22,71	3.97893
4	12,30,57,93	8,22,42,81	8,21,40,78	4.02494	12,30,57,93	8,22,42,81	8,21,40,78	4.02494
6	10,30,56,85,127,207	11,24,42,71,114,235	10,22,42,76,138,194	4.02987	9,29,54,83,127,211	8,21,40,71,110,234	8,20,42,75,137,193	4.02988
8	7,20,31,46,63,89,120,178	8,15,24,29,50,81,125,234	8,6,14,29,3941,73,106,175,214	4.03710	8,19,28,44,64,87,116,180	7,12,24,41,55,82,123,228	8,16,29,44,66,105,174,221	4.03712
				Flower				
2	41,119	44,111	53,114	12.34354	41,119	44,111	53,114	12.34354
4	39,79,135,199	27,52,93,159	23,56,98,157	12.39484	39,79,135,199	27,52,93,159	23,56,98,157	12.39484
6	28,48,78,119,168,214	25,41,59,87,131,186	8,35,64,106,146,191	12.40939	27,47,77,119,167,213	22,41,61,87,128,184	6,34,63,99,146,192	12.40940
8	15,30,45,57,81,123,179,218	25,39,58,82,106,136,173,216	9,31,44,68,87,108,147,198	12.41604	18,29,44,58,82,124,171,216	22,41,58,77,105,136,166,205	6,27,45,65,91,118,154,199	12.41606
				Girl				
2	41,90	22,72	26,80	7.65874	41,90	22,72	26,80	7.65874
4	33,65,102,149	11,31,62,109	11,28,56,101	7.70152	33,65,102,149	11,31,62,109	11,28,56,101	7.70152
6	22,46,67,100,134,186	10,33,58,90,124,183	14,26,57,100,146,168	7.70993	23,44,68,98,132,185	10,29,59,89,122,182	11,26,55,95,144,166	7.70994
8	21,39,55,67,88,103,135,172	6,19,35,43,56,87,110,154	12,44,50,134,141,167,204,237	7.71551	18,36,52,71,90,110,132,167	8,22,30,42,61,85,117,153	11,45,51,128,152,173,209,239	7.71553
				Monarch				
2	108,172	75,135	58,113	14.98290	108,172	75,135	58,113	14.98290
4	79,115,147,186	61,86,119,169	38,61,91,141	15.00562	79,115,147,186	61,86,119,169	38,61,91,141	15.00562
6	64,86,112,141,166,202	42,65,82,101,133,179	34,47,69,92,123,164	15.01302	61,85,112,139,165,199	44,63,83,102,130,175	38,50,68,89,119,163	15.01303
8	55,73,92,111,136,154,177,207	39,54,66,86,99,120,148,190	36,49,63,75,92,116,146,175	15.01597	61,77,93,110,132,148,176,200	33,53,62,83,97,124,143,182	39,47,59,74,90,118,143,170	15.01599
				Pen				
2	61,133	48,125	49,136	13.20604	61,133	48,125	49,136	13.20604
4	45,76,112,169	34,66,101,157	29,63,102,166	13.25261	45,76,112,169	34,66,101,157	29,63,102,166	13.25261
6	38,57,82,109,144,189	28,48,73,98,136,184	21,42,66,98,124,180	13.26477	35,55,77,104,141,187	26,50,71,96,134,184	22,43,72,97,128,183	13.26478
8	33,50,64,88,106,135,168,201	26,41,59,75,102,120,152,196	19,30,56,73,94,119,151,200	13.27000	31,48,67,85,105,132,165,202	24,42,60,78,97,123,155,192	17,32,54,76,96,115,154,201	13.27001
				Pepper				
2	87,153	22,104	21,74	16.40133	87,153	22,104	21,74	16.40133
4	62,102,137,174	10,39,85,156	15,52,83,133	16.45113	62,102,137,174	10,39,85,156	15,52,83,133	16.45113
6	49,82,108,133,164,191	11,34,62,100,152,185	6,26,55,84,115,166	16.46414	51,82,113,135,163,190	9,35,65,104,149,189	8,30,56,81,116,172	16.46415
8	48,72,99,118,136,157,178,197	9,25,44,69,101,126,170,201	10,28,45,64,84,110,160,189,196	16.46921	44,73,98,113,130,156,177,198	5,22,45,68,94,132,161,194	6,25,42,65,83,120,170,192	16.46923
				Soccer				
2	64,126	42,97	42,113	13.11371	64,126	42,97	42,113	13.11371
4	43,79,123,165	30,63,105,155	25,60,99,150	13.15363	43,79,123,165	30,63,105,155	25,60,99,150	13.15363
6	39,62,94,127,160,191	22,45,72,97,125,169	21,48,79,104,141,193	13.16533	38,62,91,125,156,187	23,43,67,96,126,168	22,46,77,104,140,192	13.16534
8	35,55,71,96,124,145,166,198	19,38,59,79,106,121,145,177	16,30,50,65,87,105,133,173	13.17064	33,49,72,95,125,146,165,196	21,39,60,82,103,123,142,176	15,29,44,67,86,106,123,169	13.17066
				Test				
2	80,137	83,140	67,132	16.22951	80,137	83,140	67,132	16.22951
4	55,88,122,167	40,70,97,143	39,65,100,155	16.25759	55,88,122,167	40,70,97,143	39,65,100,155	16.25759
6	41,70,90,124,158,190	37,65,95,119,152,185	33,50,69,92,126,169	16.26695	43,70,95,123,157,192	38,66,90,116,151,182	30,51,68,91,127,170	16.26696
8	38,64,78,98,110,134,164,198	37,60,72,90,104,127,155,188	30,46,63,83,106,132,159,184	16.27101	39,62,77,95,113,128,165,199	35,56,75,91,112,133,162,190	28,48,63,82,104,128,157,185	16.27103
				Yacht				
2	60,133	55,125	53,127	15.87338	60,133	55,125	53,127	15.87338
4	44,80,119,166	28,56,92,139	25,55,99,154	15.91058	44,80,119,166	28,56,92,139	25,55,99,154	15.91058
6	31,51,83,112,141,179	26,51,77,97,128,170	21,43,68,94,126,164	15.92185	30,52,82,108,141,178	25,48,74,95,126,167	20,41,64,90,122,162	15.92186
8	30,43,66,95,114,135,162,187	23,42,63,83,102,122,148,178	22,31,52,78,99,125,150,180	15.92641	28,48,70,89,110,137,162,186	22,40,53,80,98,121,145,171	18,34,53,74,92,124,148,179	15.92644

Table 9: Comparison of optimal PSNR (dB) and SSIM values obtained by IGSO, GSO, APSO, and SaDE algorithms using MCE.

Image	m	IGSO		GSO		APSO		SaDE	
		PSNR	SSIM	PSNR	SSIM	PSNR	SSIM	PSNR	SSIM
Airplane	2	10.0178	0.7896	10.0178	0.7896	10.0178	0.7896	10.0178	0.7896
	4	10.0216	0.8394	10.0216	0.8394	10.0216	0.8394	10.0216	0.8394
	6	**10.0381**	**0.8794**	10.0311	0.8708	10.0232	0.8617	10.0258	0.8659
	8	**10.0641**	**0.9308**	10.0592	0.9248	10.0516	0.9101	10.0548	0.9159
Couple	2	27.0372	0.8270	27.0372	0.8270	27.0372	0.8270	27.0372	0.8270
	4	27.0478	0.8860	27.0478	0.8860	27.0478	0.8860	27.0478	0.8860
	6	**27.0568**	**0.9128**	25.0526	0.9032	27.0499	0.8929	27.0512	0.8973
	8	**27.0613**	**0.9460**	25.0588	0.9343	27.0523	0.9290	27.0562	0.9311
Flower	2	19.3352	0.8696	19.3352	0.8696	19.3352	0.8696	19.3352	0.8696
	4	19.3369	0.9037	19.3369	0.9037	19.3369	0.9037	19.3369	0.9037
	6	**19.3385**	**0.9385**	19.3376	0.9243	19.3370	0.9159	19.3373	0.9213
	8	**19.3439**	**0.9679**	19. 3417	0.9538	19.3389	0.9337	19.3402	0.9446
Girl	2	24.0684	0.7274	24.0684	0.7274	24.0684	0.7274	24.0684	0.7274
	4	24.0725	0.8369	24.0725	0.8369	24.0725	0.8369	24.0725	0.8369
	6	**24.0761**	**0.8740**	24.0749	0.8649	27.0732	0.8568	24.0740	0.8614
	8	**24.0844**	**0.9192**	24.0824	0.9069	24.0771	0.8903	24.0792	0.8971
Monarch	2	19.4791	0.7605	19.4791	0.7605	19.4791	0.7605	19.4791	0.7605
	4	19.4851	0.8648	19.4851	0.8648	19.4851	0.8648	19.4851	0.8648
	6	**19.4867**	**0.9208**	19.4862	0.9121	19.4850	0.9032	19.4855	0.9085
	8	**19.4939**	**0.9524**	19.4902	0.9408	19,4879	0.9264	19.4893	0.9336
Pen	2	19.8970	0.8281	19.8970	0.8281	19.8970	0.8281	19.8970	0.8281
	4	19.8992	0.8878	19.8992	0.8878	19.8992	0.8878	19.8992	0.8878
	6	**19.8996**	**0.9317**	19.8993	0.9244	19.8987	0.9117	19.8991	0.9184
	8	**19.9052**	**0.9637**	19.9021	0.9546	19.8994	0.9396	19.9010	0.9441
Pepper	2	18.1823	0.8189	18.1823	0.8189	18.1823	0.8189	18.1823	0.8189
	4	18.1849	0.8460	18.1849	0.8460	18.1849	0.8460	18.1849	0.8460
	6	**18.1867**	**0.9021**	18.1860	0.8967	18.1848	0.8815	18.1853	0.8913
	8	**18.1897**	**0.9483**	18.1883	0.9377	18.1860	0.9239	18.1875	0.9314
Soccer	2	20.3415	0.8016	20.3415	0.8016	20.3415	0.8016	20.3415	0.8016
	4	20.3378	0.8512	20.3378	0.8512	20.3378	0.8512	20.3378	0.8512
	6	**20.3471**	**0.9071**	20.3442	0.8992	20.3496	0.8869	20.3411	0.8983
	8	**20.3499**	**0.9560**	20.3475	0.9477	20.3420	0.9298	20.3448	0.9329
Test	2	18.5027	0.7658	18.5027	0.7658	18.5027	0.7658	18.5027	0.7658
	4	18.5155	0.8560	18.5155	0.8560	18.5155	0.8560	18.5155	0.8560
	6	**18.5157**	**0.9021**	18.5154	0.8938	18.5153	0.8802	18.5154	0.8859
	8	**18.5168**	**0.9533**	18.5161	0.9486	18.5156	0.9372	18.5158	0.9400
Yacht	2	18.5135	0.8195	18.5135	0.8195	18.5135	0.8195	18.5135	0.8195
	4	18.5172	0.8611	18.5172	0.8611	18.5172	0.8611	18.5172	0.8611
	6	**18.5188**	**0.9150**	18.5179	0.9021	18.5174	0.8851	18.5177	0.8960
	8	**18.5203**	**0.9608**	18.5186	0.9454	18.5178	0.9287	18.5182	0.9342

The parameter values of PSNR (dB) and SSIM value are shown in Table 9. Figures 5 and 6 give the multilevel thresholding segmented results at 2, 4, 6, and 8 levels of thresholding using IGSO algorithm based on minimum cross entropy for ten test color images, respectively.

4.3. Comparison of the Segmented Performance. In this paper, the results of IGSO algorithm based on Otsu and MCE have been compared with basic GSO algorithm and two other well-known optimization algorithms. For the Otsu fitness function, it can be clearly seen from Tables 4 and 5 that the improved GSO algorithm offers superior optimal thresholds and objective values in comparison with GSO, APSO, and SaDE algorithms when the number of thresholds is more than 4. From Tables 7 and 8, it is easy to deduce that the optimal thresholds and objective values of multilevel color image

Table 10: Comparison of optimal PSNR (dB) and SSIM values obtained by IGSO and GSO algorithms using OTSU and MCE.

Image	m	PSNR (Otsu)		PSNR (MCE)		SSIM (Otsu)		SSIM (MCE)	
		IGSO	GSO	IGSO	GSO	IGSO	GSO	IGSO	GSO
Airplane	2	10.0144	10.0144	10.0178	10.0178	0.7740	0.7740	0.7896	0.7896
	4	10.0188	10.0188	10.0216	10.0216	0.8246	0.8246	0.8394	0.8394
	6	10.0300	10.0263	**10.0381**	10.0311	0.8575	0.8398	**0.8794**	0.8708
	8	10.3589	10.3524	**10.3641**	10.0592	0.9134	0.9029	**0.9308**	0.9248
Couple	2	27.0382	27.0382	27.0372	27.0372	0.8025	0.8025	0.8270	0.8270
	4	27.0470	27.0470	27.0478	27.0478	0.8830	0.8830	0.8860	0.8860
	6	27.0579	27.0518	27.0568	25.0526	0.9143	0.9093	**0.9128**	0.9032
	8	27.0602	27.0559	**27.0613**	25.0588	0.9427	0.9362	**0.9460**	0.9343
Flower	2	19.3175	19.3175	**19.3352**	19.3352	0.8460	0.8460	0.8696	0.8696
	4	19.3280	19.3280	19.3369	19.3369	0.9040	0.9040	0.9037	0.9037
	6	19.3286	19.3278	**19.3385**	19.3376	0.9372	0.9340	**0.9385**	0.9243
	8	20.3152	20.2937	**20.3439**	19. 3417	0.9604	0.9549	**0.9679**	0.9538
Girl	2	24.0610	24.0610	24.0684	24.0684	0.7112	0.7112	0.7274	0.7274
	4	24.0734	24.0734	24.0725	24.0725	0.8011	0.8011	0.8369	0.8369
	6	24.0758	24.0766	**24.0761**	24.0749	0.8584	0.8546	**0.8740**	0.8649
	8	24.0824	24.0802	**24.0844**	24.0824	0.9094	0.8982	**0.9192**	0.9069
Monarch	2	19.4727	19.4727	19.4791	19.4791	0.7658	0.7658	0.7605	0.7605
	4	19.4767	19.4767	19.4851	19.4851	0.8589	0.8589	0.8648	0.8648
	6	19.4785	19.4778	**19.4867**	19.4862	0.9155	0.9116	**0.9208**	0.9121
	8	19.4941	19.4879	**19.4939**	19.4902	0.9454	0.9387	**0.9524**	0.9408
Pen	2	19.8912	19.8912	19.8970	19.8970	0.8420	0.8420	0.8281	0.8281
	4	19.8935	19.8935	19.8992	19.8992	0.8791	0.8791	0.8878	0.8878
	6	19.8983	19.8961	**19.8994**	19.8993	0.9330	0.9238	**0.9317**	0.9244
	8	19.9014	19.9001	**19.9052**	19.9021	0.9629	0.9581	**0.9637**	0.9546
Pepper	2	18.1771	18.1771	18.1823	18.1823	0.8046	0.8046	0.8189	0.8189
	4	18.1789	18.1789	18.1849	18.1849	0.8384	0.8384	0.8460	0.8460
	6	18.1856	18.1825	**18.1857**	18.1860	0.9004	0.8976	**0.9021**	0.8967
	8	18.1891	18.1836	**18.1897**	18.1883	0.9476	0.9302	**0.9483**	0.9377
Soccer	2	20.3329	20.3329	20.3415	20.3415	0.8088	0.8088	0.8016	0.8016
	4	20.3368	20.3368	20.3378	20.3378	0.8570	0.8570	0.8512	0.8512
	6	20.3466	20.3421	**20.3471**	20.3442	0.9023	0.8931	**0.9071**	0.8992
	8	20.3474	20.3437	**20.3499**	20.3475	0.9529	0.9493	**0.9560**	0.9477
Test	2	18.5023	18.5023	18.5027	18.5027	0.7611	0.7611	0.7658	0.7658
	4	18.5081	18.5081	18.5155	18.5155	0.8508	0.8508	0.8560	0.8560
	6	18.5106	18.5091	18.5157	18.5154	0.9017	0.8959	0.9021	0.8938
	8	18.5144	18.5120	18.5168	18.5161	0.9446	0.9274	0.9533	0.9486
Yacht	2	18.5073	18.5073	18.5135	18.5135	0.8133	0.8133	0.8195	0.8195
	4	18.5083	18.5083	18.5172	18.5172	0.8503	0.8503	0.8611	0.8611
	6	18.5090	18.5086	**18.5175**	18.5179	0.9035	0.8910	**0.9150**	0.9021
	8	18.5164	18.5122	**18.5203**	18.5186	0.9542	0.9389	**0.9608**	0.9454

thresholding segmentation using minimum cross entropy for all the test images are better than GSO, APSO, and SaDE algorithms.

The parameters of peak signal to noise ratio (PSNR) and structural similarity (SSIM) index are introduced to evaluate the quality of segmented images. Tables 6 and 9 show that PSNR and SSIM values obtained with IGSO algorithm are higher than those produced by the other algorithms. The PSNR and SSIM values obtained by IGSO and GSO algorithms using Otsu's and MCE methods are presented in Table 10. For the same color test image and number of thresholds (m), the IGSO algorithm based on the minimum cross entropy method has higher PSNR and SSIM values than Otsu's method. After the analysis of results, it is found that

IGSO algorithm based on the minimum cross entropy has better quality of segmented image than the other algorithms for each color test image.

Moreover, the convergence curves for IGSO, GSO, APSO, and SaDE algorithms of ten test color images using Otsu's method have been shown in Figure 7 for 8-level thresholding. It can be clearly observed from these figures that the IGSO algorithm needs less iterations to obtain optimal segmentation results and has better convergence property than GSO, APSO, and SaDE algorithms for multilevel color image thresholding segmentation.

5. Conclusions

In this paper, a new multilevel color image thresholding segmentation method based on improved glowworm swarm optimization (IGSO) algorithm is presented. The presented method utilized Otsu's method and minimum cross entropy as the fitness functions criteria and is tested on ten color test images for $m = 2, 4, 6$, and 8. The results obtained by IGSO algorithm are compared with those obtained by GSO, APSO, and SaDE algorithms and the segmentation performance of these methods was evaluated in terms of the optimal threshold values, optimal objective values, PSNR values, and SSIM values. Finally, the convergence curves using minimum cross entropy are drawn of ten test color images for $m = 8$. The comparative results show that the improved GSO algorithm is superior to the GSO, APSO, and SaDE algorithms for multilevel color image thresholding problem. Furthermore, the quality of segmented image of the IGSO algorithm using minimum cross entropy outperforms the IGSO algorithm using Otsu's method in terms of PSNR and SSIM. The further work will include introduction of the other fitness criteria for multilevel thresholding segmentation. In addition, the IGSO algorithm is also applied to the other complex problems.

Competing Interests

The authors declare that there is no conflict of interests regarding the publication of this paper.

Acknowledgments

This work was supported by the National Nature Science Foundation of China (no. 51204077) and the Nature Science Foundation of Kunming University of Science and Technology (no. 2014-9-x-8).

References

[1] G. S. Linda and C. S. George, *Computer Vision*, Prentice Hall, Upper Saddle River, NJ, USA, 1st edition, 2001.

[2] L. Barghout and L. Lee, "Perceptual information processing system," U.S. Patent Application 10/618,543, 2003.

[3] D. L. Pham, C. Xu, and J. L. Prince, "Current methods in medical image segmentation," *Annual Review of Biomedical Engineering*, vol. 2, pp. 315–337, 2000.

[4] J. A. Delmerico, P. David, and J. J. Corso, "Building facade detection, segmentation, and parameter estimation for mobile robot localization and guidance," in *Proceedings of the IEEE/RSJ International Conference on Intelligent Robots and Systems (IROS '11)*, pp. 1632–1639, IEEE, San Francisco, Calif, USA, September 2011.

[5] F. Yan, H. Zhang, and C. R. Kube, "A multistage adaptive thresholding method," *Pattern Recognition Letters*, vol. 26, no. 8, pp. 1183–1191, 2005.

[6] J. Fan, M. Han, and J. Wang, "Single point iterative weighted fuzzy C-means clustering algorithm for remote sensing image segmentation," *Pattern Recognition*, vol. 42, no. 11, pp. 2527–2540, 2009.

[7] N. Otsu, "A threshold selection method from gray-level histograms," *IEEE Transactions on Systems, Man, and Cybernetics*, vol. 9, no. 1, pp. 962–966, 1979.

[8] W.-H. Tsai, "Moment-preserving thresholding: a new approach," *Computer Vision, Graphics, & Image Processing*, vol. 29, no. 3, pp. 377–393, 1985.

[9] J. Kittler and J. Illingworth, "Minimum error thresholding," *Pattern Recognition*, vol. 19, no. 1, pp. 41–47, 1986.

[10] C. H. Li and C. K. Lee, "Minimum cross entropy thresholding," *Pattern Recognition*, vol. 26, no. 4, pp. 617–625, 1993.

[11] M. Sezgin and B. Sankur, "Survey over image thresholding techniques and quantitative performance evaluation," *Journal of Electronic Imaging*, vol. 13, no. 1, pp. 146–168, 2004.

[12] S. Wang, F.-L. Chung, and F. Xiong, "A novel image thresholding method based on Parzen window estimate," *Pattern Recognition*, vol. 41, no. 1, pp. 117–129, 2008.

[13] D.-Y. Huang and C.-H. Wang, "Optimal multi-level thresholding using a two-stage Otsu optimization approach," *Pattern Recognition Letters*, vol. 30, no. 3, pp. 275–284, 2009.

[14] G. Beni and J. Wang, "Swarm intelligence in cellular robotic systems," in *Robots and Biological Systems: Towards a New Bionics?* P. Dario, G. Sandini, and P. Aebischer, Eds., vol. 102 of *NATO ASI Series*, pp. 703–712, Springer, Berlin, Germany, 1993.

[15] W.-B. Tao, J.-W. Tian, and J. Liu, "Image segmentation by three-level thresholding based on maximum fuzzy entropy and genetic algorithm," *Pattern Recognition Letters*, vol. 24, no. 16, pp. 3069–3078, 2003.

[16] M. Awad, K. Chehdi, and A. Nasri, "Multicomponent image segmentation using a genetic algorithm and artificial neural network," *IEEE Geoscience and Remote Sensing Letters*, vol. 4, no. 4, pp. 571–575, 2007.

[17] P.-Y. Yin, "Multilevel minimum cross entropy threshold selection based on particle swarm optimization," *Applied Mathematics and Computation*, vol. 184, no. 2, pp. 503–513, 2007.

[18] M. Maitra and A. Chatterjee, "A hybrid cooperative-comprehensive learning based PSO algorithm for image segmentation using multilevel thresholding," *Expert Systems with Applications*, vol. 34, no. 2, pp. 1341–1350, 2008.

[19] B. Akay, "A study on particle swarm optimization and artificial bee colony algorithms for multilevel thresholding," *Applied Soft Computing Journal*, vol. 13, no. 6, pp. 3066–3091, 2013.

[20] M.-H. Horng, "Multilevel thresholding selection based on the artificial bee colony algorithm for image segmentation," *Expert Systems with Applications*, vol. 38, no. 11, pp. 13785–13791, 2011.

[21] Y. Zhang and L. Wu, "Optimal multi-level thresholding based on maximum Tsallis entropy via an artificial bee colony approach," *Entropy*, vol. 13, no. 4, pp. 841–859, 2011.

[22] A. K. Bhandari, A. Kumar, and G. K. Singh, "Modified artificial bee colony based computationally efficient multilevel thresholding for satellite image segmentation using Kapur's, Otsu and Tsallis functions," *Expert Systems with Applications*, vol. 42, no. 3, pp. 1573–1601, 2015.

[23] E. Cuevas, D. Zaldivar, and M. Pérez-Cisneros, "A novel multi-threshold segmentation approach based on differential evolution optimization," *Expert Systems with Applications*, vol. 37, no. 7, pp. 5265–5271, 2010.

[24] S. Sarkar and S. Das, "Multilevel image thresholding based on 2D histogram and maximum Tsallis entropy—a differential evolution approach," *IEEE Transactions on Image Processing*, vol. 22, no. 12, pp. 4788–4797, 2013.

[25] H. V. H. Ayala, F. M. dos Santos, V. C. Mariani, and L. D. dos Santos Coelho, "Image thresholding segmentation based on a novel beta differential evolution approach," *Expert Systems with Applications*, vol. 42, no. 4, pp. 2136–2142, 2015.

[26] M. H. Horng and T. W. Jiang, "Multilevel image thresholding selection based on the firefly algorithm," in *Proceedings of the Ubiquitous Intelligence & Computing and 7th International Conference on Autonomic & Trusted Computing (UIC/ATC '10)*, pp. 58–63, Xian, China, October 2010.

[27] M.-H. Horng and R.-J. Liou, "Multilevel minimum cross entropy threshold selection based on the firefly algorithm," *Expert Systems with Applications*, vol. 38, no. 12, pp. 14805–14811, 2011.

[28] S. Agrawal, R. Panda, S. Bhuyan, and B. K. Panigrahi, "Tsallis entropy based optimal multilevel thresholding using cuckoo search algorithm," *Swarm and Evolutionary Computation*, vol. 11, pp. 16–30, 2013.

[29] A. K. Bhandari, V. K. Singh, A. Kumar, and G. K. Singh, "Cuckoo search algorithm and wind driven optimization based study of satellite image segmentation for multilevel thresholding using Kapur's entropy," *Expert Systems with Applications*, vol. 41, no. 7, pp. 3538–3560, 2014.

[30] D. Oliva, E. Cuevas, G. Pajares, D. Zaldivar, and V. Osuna, "A Multilevel thresholding algorithm using electromagnetism optimization," *Neurocomputing*, vol. 139, pp. 357–381, 2014.

[31] K. Hammouche, M. Diaf, and P. Siarry, "A multilevel automatic thresholding method based on a genetic algorithm for a fast image segmentation," *Computer Vision and Image Understanding*, vol. 109, no. 2, pp. 163–175, 2008.

[32] S. Manikandan, K. Ramar, M. W. Iruthayarajan, and K. G. Srinivasagan, "Multilevel thresholding for segmentation of medical brain images using real coded genetic algorithm," *Measurement*, vol. 47, no. 1, pp. 558–568, 2014.

[33] E. Cuevas, F. Sención, D. Zaldivar, M. Pérez-Cisneros, and H. Sossa, "A multi-threshold segmentation approach based on artificial bee colony optimization," *Applied Intelligence*, vol. 37, no. 3, pp. 321–336, 2012.

[34] K. Hanbay and M. F. Talu, "Segmentation of SAR images using improved artificial bee colony algorithm and neutrosophic set," *Applied Soft Computing Journal*, vol. 21, pp. 433–443, 2014.

[35] M. Ma, J. Liang, M. Guo, Y. Fan, and Y. Yin, "SAR image segmentation based on artificial bee colony algorithm," *Applied Soft Computing Journal*, vol. 11, no. 8, pp. 5205–5214, 2011.

[36] T. Hassanzadeh, H. Vojodi, and A. M. E. Moghadam, "An image segmentation approach based on maximum variance intra-cluster method and firefly algorithm," in *Proceedings of the 7th International Conference on Natural Computation (ICNC '11)*, pp. 1817–1821, IEEE, Shanghai, China, July 2011.

[37] P. Zingaretti, G. Tascini, and L. Regini, "Optimising the color image segmentation," in *VIII Convegno dell Associazione Italiana per l'Intelligenza Artificiale*, pp. 1–8, September 2002.

[38] N. S. M. Raja, S. A. Sukanya, and Y. Nikita, "Improved PSO based multi-level thresholding for cancer infected breast thermal images using Otsu," *Procedia Computer Science*, vol. 48, pp. 524–529, 2015.

[39] S. Sarkar, S. Das, and S. S. Chaudhuri, "A multilevel color image thresholding scheme based on minimum cross entropy and differential evolution," *Pattern Recognition Letters*, vol. 54, pp. 27–35, 2015.

[40] S. Dey, S. Bhattacharyya, and U. Maulik, "New quantum inspired meta-heuristic techniques for multi-level colour image thresholding," *Applied Soft Computing*, vol. 46, pp. 677–702, 2016.

[41] V. Rajinikanth and M. S. Couceiro, "RGB histogram based color image segmentation using Firefly Algorithm," *Procedia Computer Science*, vol. 46, pp. 1449–1457, 2015.

[42] T. Kurban, P. Civicioglu, R. Kurban, and E. Besdok, "Comparison of evolutionary and swarm based computational techniques for multilevel color image thresholding," *Applied Soft Computing*, vol. 23, pp. 128–143, 2014.

[43] K. N. Krishnanand and D. Ghose, "Detection of multiple source locations using a glowworm metaphor with applications to collective robotics," in *Proceedings of the IEEE Swarm Intelligence Symposium (SIS '05)*, pp. 87–94, Pasadena, Calif, USA, June 2005.

[44] K. N. Krishnanand and D. Ghose, "Glowworm swarm based optimization algorithm for multimodal functions with collective robotics applications," *Multiagent and Grid Systems*, vol. 2, no. 3, pp. 209–222, 2006.

[45] K. N. Krishnanand and D. Ghose, "Glowworm swarm optimization for simultaneous capture of multiple local optima of multimodal functions," *Swarm Intelligence*, vol. 3, no. 2, pp. 87–124, 2009.

[46] K. N. Krishnanand and D. Ghose, "Theoretical foundations for rendezvous of glowworm-inspired agent swarms at multiple locations," *Robotics and Autonomous Systems*, vol. 56, no. 7, pp. 549–569, 2008.

[47] W.-H. Liao, Y. Kao, and Y.-S. Li, "A sensor deployment approach using glowworm swarm optimization algorithm in wireless sensor networks," *Expert Systems with Applications*, vol. 38, no. 10, pp. 12180–12188, 2011.

[48] B. Wu, C. Qian, W. Ni, and S. Fan, "The improvement of glowworm swarm optimization for continuous optimization problems," *Expert Systems with Applications*, vol. 39, no. 7, pp. 6335–6342, 2012.

[49] D. N. Jayakumar and P. Venkatesh, "Glowworm swarm optimization algorithm with topsis for solving multiple objective environmental economic dispatch problem," *Applied Soft Computing*, vol. 23, pp. 375–386, 2014.

[50] L. Qifang, O. Zhe, C. Xin, and Z. Yongquan, "A multilevel threshold image segmentation algorithm based on glowworm swarm optimization," *Journal of Computational Information Systems*, vol. 10, no. 4, pp. 1621–1628, 2014.

[51] M. H. Horng, "Multilevel image thresholding with glowworm swam optimization algorithm based on the minimum cross entropy," *Advances in Information Sciences and Service Sciences*, vol. 5, no. 10, pp. 1290–1298, 2013.

[52] Z.-H. Zhan, J. Zhang, Y. Li, and H. S.-H. Chung, "Adaptive particle swarm optimization," *IEEE Transactions on Systems, Man, and Cybernetics, Part B: Cybernetics*, vol. 39, no. 6, pp. 1362–1381, 2009.

[53] A. K. Qin and P. N. Suganthan, "Self-adaptive differential evolution algorithm for numerical optimization," in *Proceedings of*

the IEEE Congress on Evolutionary Computation (CEC '05), vol. 2, pp. 1785–1791, IEEE, Edinburgh, Scotland, September 2005.

[54] K. N. Krishnanand and D. Ghose, "Glowworm swarm optimisation: a new method for optimising multi-modal functions," *International Journal of Computational Intelligence Studies*, vol. 1, no. 1, pp. 93–119, 2009.

[55] Z. Wang, A. C. Bovik, H. R. Sheikh, and E. P. Simoncelli, "Image quality assessment: from error visibility to structural similarity," *IEEE Transactions on Image Processing*, vol. 13, no. 4, pp. 600–612, 2004.

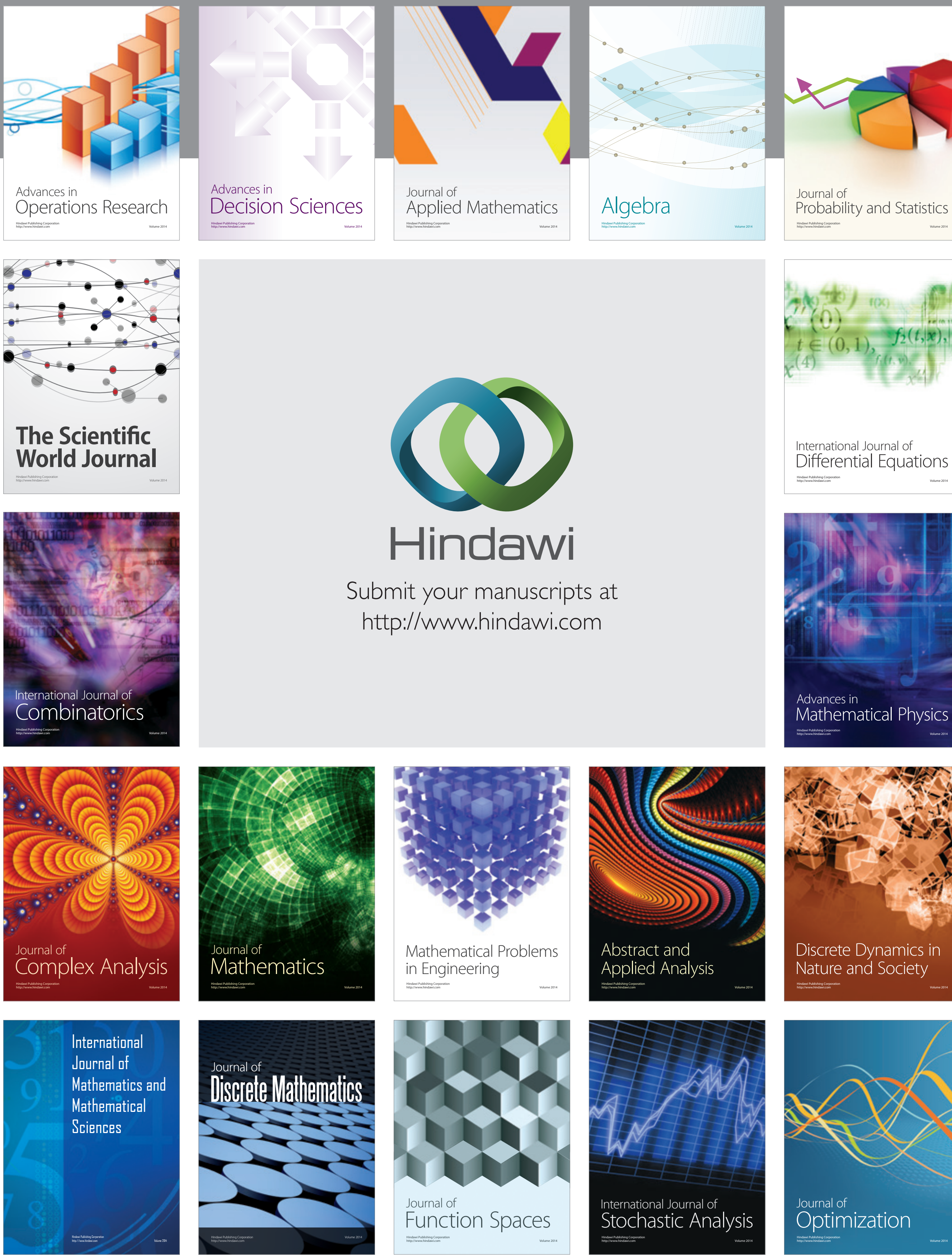

Advances in Operations Research
Advances in Decision Sciences
Journal of Applied Mathematics
Algebra
Journal of Probability and Statistics
The Scientific World Journal
Hindawi
Submit your manuscripts at
http://www.hindawi.com
International Journal of Differential Equations
International Journal of Combinatorics
Advances in Mathematical Physics
Journal of Complex Analysis
Journal of Mathematics
Mathematical Problems in Engineering
Abstract and Applied Analysis
Discrete Dynamics in Nature and Society
International Journal of Mathematics and Mathematical Sciences
Journal of Discrete Mathematics
Journal of Function Spaces
International Journal of Stochastic Analysis
Journal of Optimization